NONLINEAR-FM WAVEFORM DESIGN PROCEDURE

Shuozhong Wang
Mark Grabb
James Poplawski

COMMUNICATIONS & SIGNAL PROCESSING LABORATORY
Department of Electrical Engineering and Computer Science
The University of Michigan
Ann Arbor, Michigan 48109

November 1993

Acknowledgements

Abstract

A nonlinear FM waveform with desirable time resolution and sidelobe level properties can be constructed to drive the ATOC transducer at maximum power. This report describes the procedure for constructing an input voltage waveform that will result in an output pressure waveform with a specified power spectrum. This procedure can be used as the main routine within an iterative program to design a waveform with respect to time resolution, sidelobe level, and total transmitted power trade offs.

1.0 Introduction

Our goal is to design a chirped FM waveform[1] with a specified power spectrum for the Alliant Transducer. What makes this problem interesting is the waveform is designed so that the transducer delivers maximum instantaneous power. To deliver full power, the chirped waveform is amplitude modulated according to the constraints of the transducer. Therefore, this amplitude modulation is fixed and not free for design; however, the amplitude modulation will be slightly altered for good reason. The frequency modulation is free for design. The frequency modulation will be designed to force the waveform to have a power spectrum that corresponds to a chosen shape with low time-domain side lobes. The raised-cosine spectral shape is used. To accomplish this, a non-linear frequency modulated waveform with amplitude modulation will be designed.

The design procedure described in this report works well. The designed chirped FM waveform successfully delivers full instantaneous power for most of the signal period. It has a power spectrum identical to a raised-cosine shape. As a result, the time resolution and sidelobe levels of the received matched filtered waveform reach the specifications of the desired waveform having a raised-cosine power spectrum.

In the next section the design procedure is outlined. In the following and final section, the design procedure is detailed by way of an example.

2.0 Outline of Design Procedure

The design procedure is outlined by stepping through Table 1 on page 3. The Alliant Transducer is driven by a voltage waveform and delivers a sound pressure

---

[1]A chirp is a frequency modulated signal segment with monotone frequency change, such as a simple whistle signal

1

waveform into the ocean. The complete system consists of a cable (50 nautical miles), tuner, and the transducer (located at a 1000 m depth). The system is modelled as a linear system. The designed chirped FM waveform will start with a low instantaneous frequency, f_L, of 60 Hz and chirp to a final high instantaneous frequency, f_H, of 94 Hz, for a total frequency excursion of 34 Hz. The center frequency is 77 Hz. The period of the chirp, T, is 29 9/35 seconds. The sampling frequency used is 280 Hz, requiring a total number of points equal to 8192.

To begin the design, the transfer function of this linear system is computed. Internal to the transducer, there are two constraints (as of 5 August 1993). The rms voltage across the ceramic stack cannot exceed 4010 volts. Also a certain peak stress cannot exceed 3206 psi. Based on these constraints, the maximum allowable input voltage as a function of frequency is computed. Call this A(f). For reasons described in Section 3, A(f) is smoothed and levelled to form B(f). B(f) is used to amplitude modulate a linear-FM chirp. This leans heavily on the assumption[2] that the steady-state frequency, the argument of B(f), equals the instantaneous frequency of the chirp, f_{inst}.

An AM linear-FM chirp, $s_1(t)$, is transformed into the frequency domain and multiplied by the linear system transfer function to compute the output pressure spectrum, $P_1(f)$ and ultimately the output power spectrum, $|P_1(f)|^2$.

$$s_1(t) = B(f_{inst}(t))cos(\phi_{inst}(t))$$

$$where \quad f_{inst}(t) = f_L + (f_H - f_L)t/T, \quad and \quad 2\pi(d\phi_{inst}(t)/dt) = f_{inst}(t) \quad linear \quad FM$$

[2]This is known as the quasi-steady-state assumption. In Section 3, the use of this assumption is justified

2

Table 1: Waveform Design Procedure

1. Compute System Transfer Function

2. Compute Max Input Voltage, smooth and level: B(f)

3. Form time-domain linear FM using B(f(t)) < input1 >

4. Compute pressure output of System using AM-LFM as input

5. Compute output power spectrum P2OUT1

6. Compute desired power spectrum

7. dt/df = DESIRED/P2OUT1

8. Integrate to get t(f)

9. Invert t(f) to get f(t)

10. Integrate f(t) to get phase(t)

11. Form AM-NLFM: using B(f(t)) for AM and phase(t) for NLFM: < input2 >

12. Compute output pressure spectrum: PRESSURE2

13. Ripple Removal: PRESSURE3 = sqrt(DESIRED)*exp(j*angle(PRESSURE2))

14. Find INPUT3 which produces PRESSURE3, with overshooting: < input3 >

15. Modify B(f(t)) to curb overshooting

16. Repeat steps 3 - 9, get new f(t) and a de-rippled waveform: < input4/input5 >

17. Modify f1(t) and get f(t) to remove phase discontinuity: < input6 >

18. Repeat steps 10 - 14 to get derippled, non-overshooting, phase-continuous AM-NLFM: < input7 >

19. Send INPUT7 through system and check constraints

20. Signal performance: matched filter output

Capital letters "INPUT" denotes frequency domain representation Lower-case letters "input" denotes time domain representation

3

This design causes the transducer to deliver maximum instantaneous power across the chosen frequency band. However, the resulting output power spectrum, $|P_1(f)|^2$, does not have a desirable shape.

Using the same AM, namely $B(f_{inst}(t))$, a nonlinear-FM approach is used to shape the spectrum. To accomplish this, a desired power spectrum is selected, $|D(f)|^2$, one that spans the chosen band and whose transform has low time-domain sidelobes. A raised-cosine shape is a popular choice.

The goal is to compute the input voltage waveform that will yield a waveform with the desired output power spectrum. To begin this procedure, the "time x power = energy" relation, $(dt/df)|P_1(f)|^2 = k|D(f)|^2$ is solved. The constant k is adjusted to get the desired period T. The relation is integrated to compute $t(f_{inst})$, a function defining the time a given instantaneous frequency should be transmitted.

$$t(f_{inst}) = k \int_{f_L}^{f_{inst}} |D(\sigma)|^2/|P_1(\sigma)|^2 d\sigma$$

From $t(f_{inst})$, $f_{inst}(t)$ is computed using numerical interpolation. The instantaneous phase as a function of time, $\theta_{inst}(t)$, is computed by integrating $f_{inst}(t)$.

$$\theta_{inst}(t) = 2\pi \int_0^t f_{inst}(\tau)d\tau$$

To deliver maximum instantaneous power, the input voltage waveform is amplitude modulated using $B(f_{inst}(t))$. The instantaneous phase, $\theta_{inst}(t)$ defines the desired nonlinear-FM for the input voltage waveform, that is, the input voltage waveform is

$$s_2(t) = B(f_{inst}(t))cos(\theta_{inst}(t))$$

This time-domain input voltage waveform is transformed into the frequency domain, then multiplied by the linear system transfer function to obtain the output

4

pressure spectrum. The output power spectrum has approximately the desired spectral shape; however, the error is significant when matched filter output waveforms are analyzed. To remove the error, which is a ripple, a new pressure spectrum is constructed. The designed phase, $\theta_{inst}(t)$, is maintained while the magnitude is replaced by a square-root raised-cosine. This pressure waveform will have an exact raised-cosine power spectrum by definition. The newly constructed output pressure waveform is run backward through the linear system to obtain the corresponding input voltage waveform. The input voltage waveform must be confirmed to be below the maximum allowable input voltage. In our case, the input voltage waveform overshoots the limitation at the beginning and end of the chirp. To remedy this violation, B(f) is modified so that overshooting does not occur. Once an acceptable B(f) is crafted, the design procedure is restarted using this new B(f), and at this point in the design, no overshooting will occur.

The chirp will be repeated periodically without delay. Therefore, the waveform instantaneously transitions from an instantaneous frequency of 94 to 60 Hz. It is important that the phase not be discontinuous at this juncture so that a time-domain spike does not result. Here, $f_{inst}(t)$ is extrapolated so that the beginning and end phases smoothly match, and a corresponding $\theta_{inst}(t)$ is recalculated. The procedure is continued (repeated) to construct the ripple removed pressure spectrum. This spectrum is sent backward through the system and the corresponding input voltage waveform is computed. This waveform does not overshoot the input voltage limitations, is phase continuous, and produces a pressure waveform with an exact raised-cosine power spectrum.

The output of a matched filter, an autocorrelation, is the Fourier transform of the

5

output power spectrum. The designed waveform provides the same time resolution and sidelobe levels as the desired waveform.

The design procedure is heavily dependent upon the quasi-steady-state (QSS) assumption. The QSS-based AM nonlinear-FM signal is passed through the linear system in the frequency domain, and the performance of the output sound pressure waveform, the instantaneous ceramic stack voltage and stress, and other electrical parameters within the system are examined. It is found that all the design specifications are satisfied. This is considered as a validation of the QSS approach.

3.0 Detailed Design Procedure

The chirped waveform design procedure will be described by walking through an example. The chirp will begin at $f_L = 60$ Hz, end at $f_H =94$ Hz, and last T = 29 9/35 seconds. The input voltage waveform will drive the transducer so that maximum instantaneous power is delivered for the duration of the chirp. The design procedure will cause the pressure waveform to have a raised-cosine power spectrum.

Fifty nautical miles of cable, a tuner, and the transducer, located one thousand meters underwater, are modelled as a linear system. The cable and tuner are modeled using capacitors, resistors, inductors and ideal transformers. Likewise, the mechanical parts of the transducer are modelled using a mechanical-to-electrical equivalent. The overall equivalent system circuit is simulated using an ABCD matrix approach. The magnitude and phase of the transfer function for the linear system, which is a pressure power output due to a one-volt input, is shown in Figures 1a and 1b. A signal bandwidth of 34 Hz with center frequency at 77 Hz appears reasonable. The system phase is a well-behaved slow roll of approximately 4 radians across the design bandwidth. There are two constraints within the transducer, ceramic stack voltage

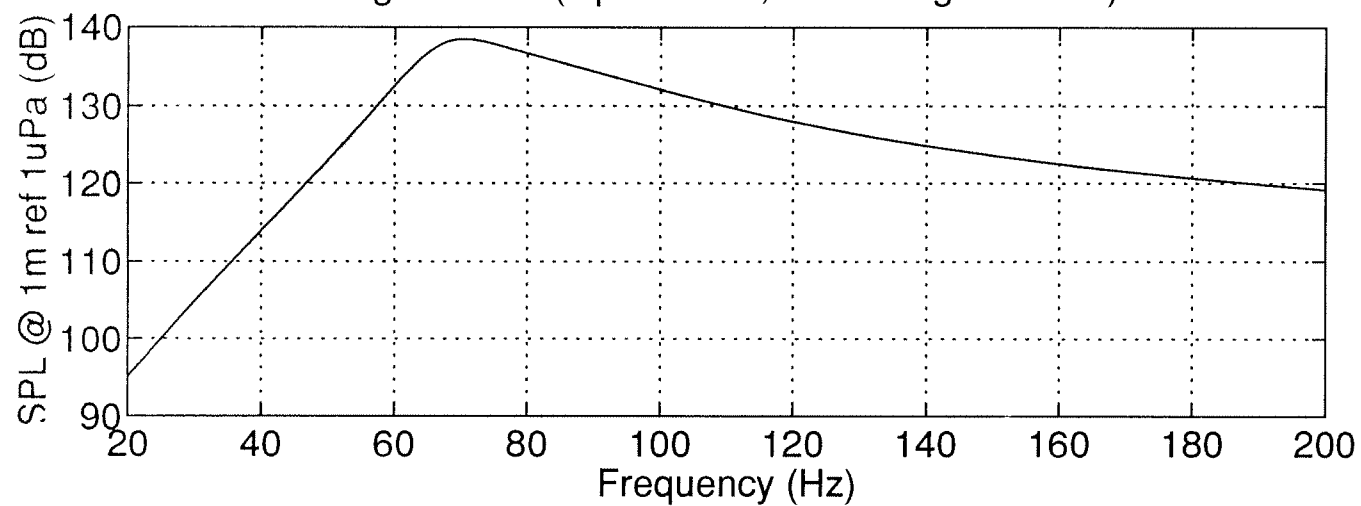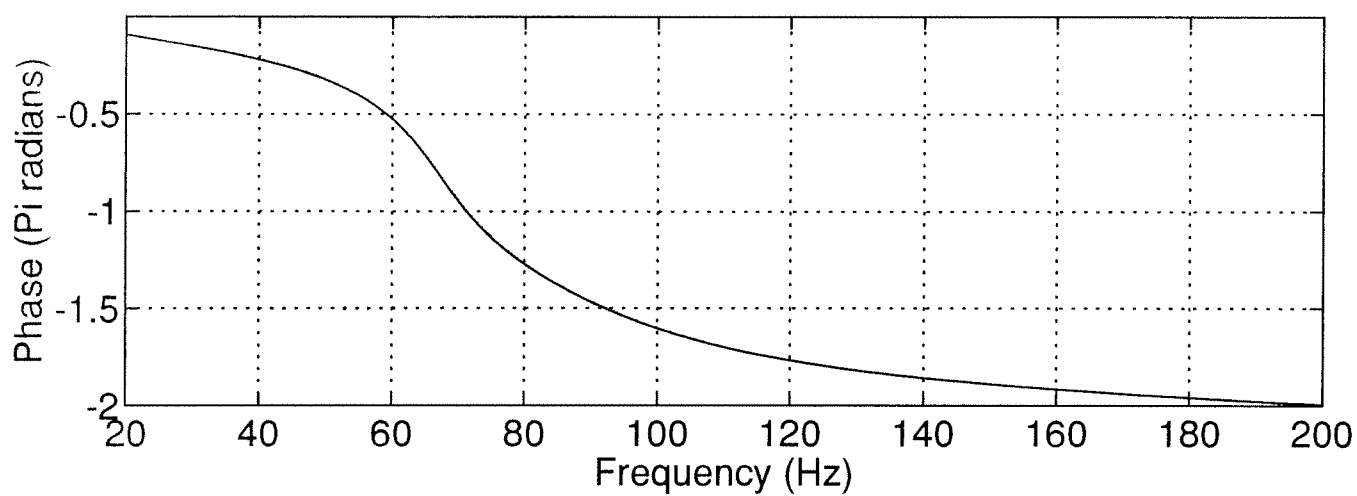Fig.1a: TVR (input=1 volt, cable length=50NM)

Fig.1b: Phase of transfer function

and stress, that limit the amplitude of the input voltage waveform. The maximum allowable voltage across the ceramic stack, E, is 4010 volts. The maximum allowable stress is 3206 psi. At each frequency, the maximum allowable input voltage is computed and shown in Figure 2. On the same plot, the resulting stack voltage and stress for each frequency are plotted for each maximum allowable input voltage. The stack voltage is the dominate constraint below 63 Hz and above 93 Hz. Thus, the stress will be the dominating constraint for the majority of the design. However, the stack voltage is the dominating constraint at the time the chirp instantaneously transitions from 94 to 60 Hz to restart the FM sweep. Within the 60 - 94 Hz frequency band of interest, the maximum allowable driving voltage as a function of frequency, A(f), is shown in Figure 3 (dashed line). If A(f) is used to form a linear-FM input voltage time-domain waveform, $s_1(t)$, and $s_1(t)$ is used to drive the transducer, then maximum instantaneous power will be delivered by the transducer.

$$s_1(t) = A(f_{inst}(t))cos(\phi_{inst}(t))$$

$where \quad f_{inst}(t) = f_L + (f_H - f_L)t/T, \quad and \quad 2\pi(d\phi_{inst}(t)/dt) = f_{inst}(t) \quad linear \quad FM$

To justify the use of using $A(f_{inst}(t))$ to form a time-domain waveform, a brief aside is required. Since the instantaneous frequency of the chirp moves slowly with time, the input waveform is treated as a steady-state sinusoid at the input waveform's instantaneous frequency. This quasi-steady-state assumption will allow a manageable approach to the waveform design. Amplitudes as function of frequency can be converted into time-domain waveform amplitudes by relating the frequency (steady state) and the instantaneous frequency as a function of time. At the end of the design, the validity of the assumption must be checked.

8

Fig.2: Maximum allowable driving voltage

Solid: Max input voltage (V)
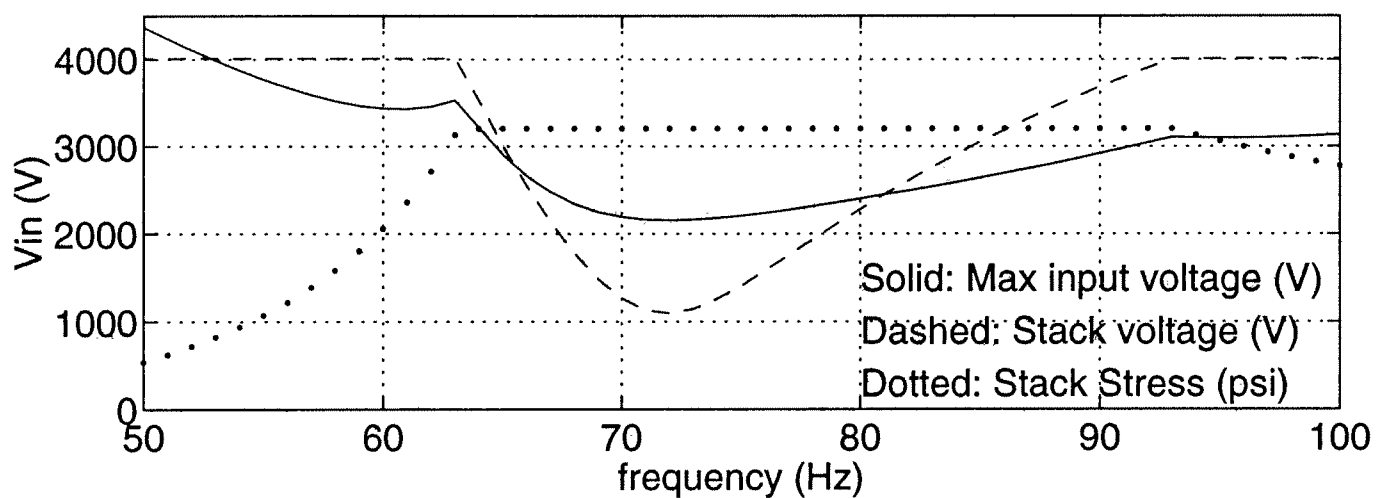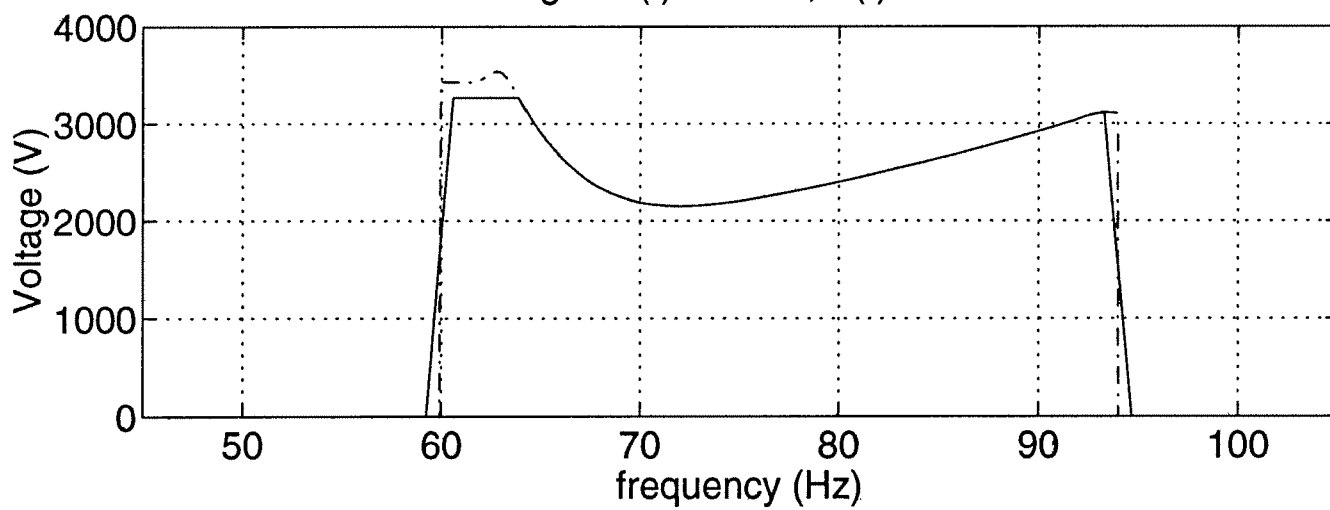Dashed: Stack voltage (V)
Dotted: Stack Stress (psi)

Fig.3: A(f):dashed; B(f):solid

There are two problems with driving the transducer with the input voltage A(f). The chirped waveform will be repeated without delay; therefore, the instantaneous frequency of the chirp will instantaneously switch from 94 Hz back to 60 Hz. To block any spurious time domain effects caused by this transition, A(f) is smoothed using a 41 point moving average. This averaging ramps the input driving voltage amplitude on and off at the 94-to-60 Hz transition. Also, the cable has a maximum allowable input voltage. The peak near 63 Hz violates this constraint. The driving voltage is levelled to remedy this violation. This smoothed and levelled input driving voltage, called B(f), is shown in Figure 3 (solid line). $B(f_{inst}(t))$ is used to amplitude modulate a linear frequency modulated input voltage waveform.

The time-domain input voltage driving waveform is

$$s_2(t) = B(f_{inst}(t))cos(\phi_{inst}(t))$$

and is shown in Figure 4a. The instantaneous phase, $f_{inst}(t)$, represents a linear frequency modulation from 60 to 94 Hz over the 29 9/35 second period. The irregularity in the waveform envelope is due to inadequate sampling for plotting purposes. In order to show the waveform envelope more accurately, the real part of the baseband analytic waveform, which is equivalent to the RF (radiated frequency) waveform, is shown in Figure 4b. The baseband waveform clearly shows the ramping on and off at each end of the signal and the required levelling during the first few seconds.

Fig.4a: AM-LFM: RF waveform
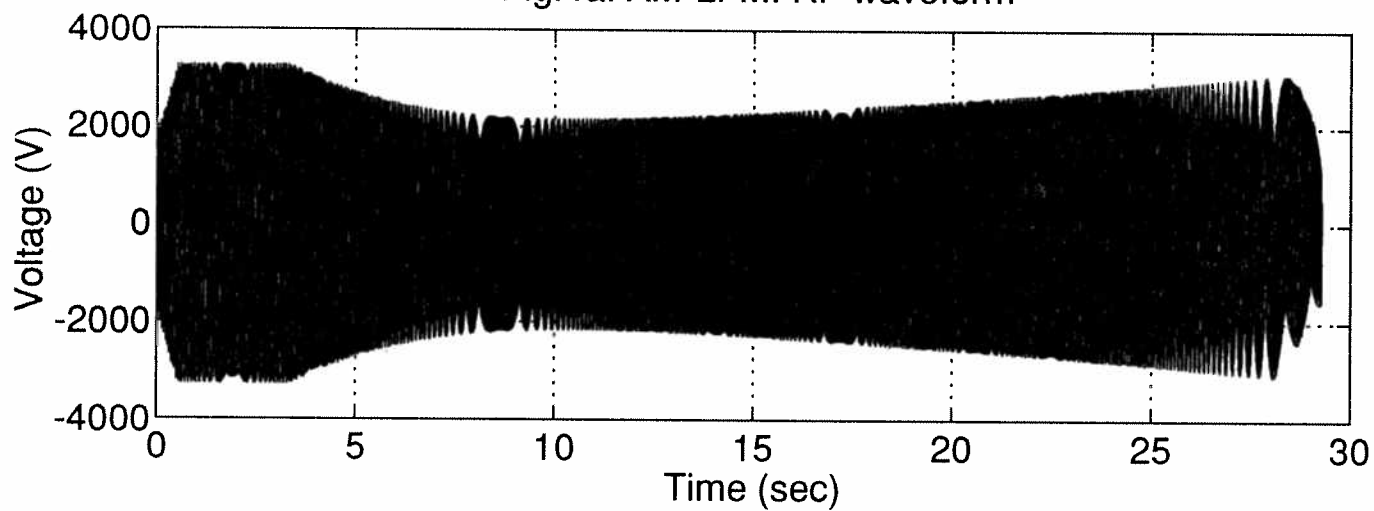
Fig.4b: AM-LFM: baseband waveform
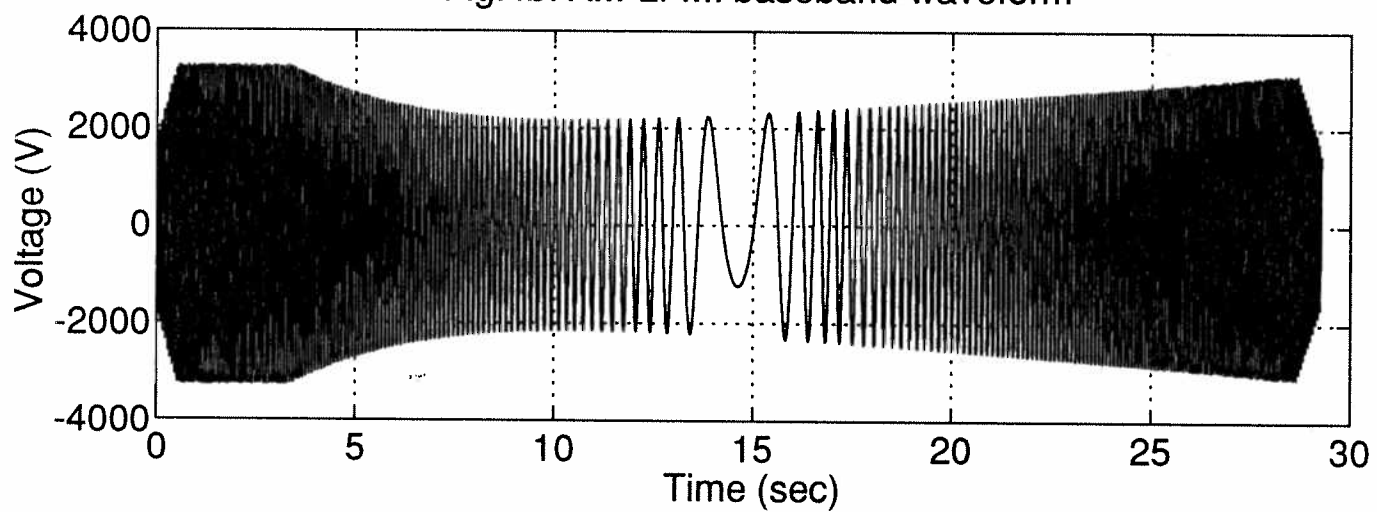
The input voltage magnitude and phase spectrum is computed using a 8192-point Fourier Transform of the time-domain input voltage driving waveform and is plotted in Figures 5a and 5b. The output spectrum is computed from the input spectrum, frequency by frequency through the linear system, while the input spectrum is obtained by Fourier transforming the AM linear-FM input waveform which is formed using $B(f_{inst}(t))$ and $f_{inst}(t)$. The magnitude of the output spectrum can be obtained by simply passing B(f) through the system, as well.

Fig.5a: Spectrum of AM-LFM
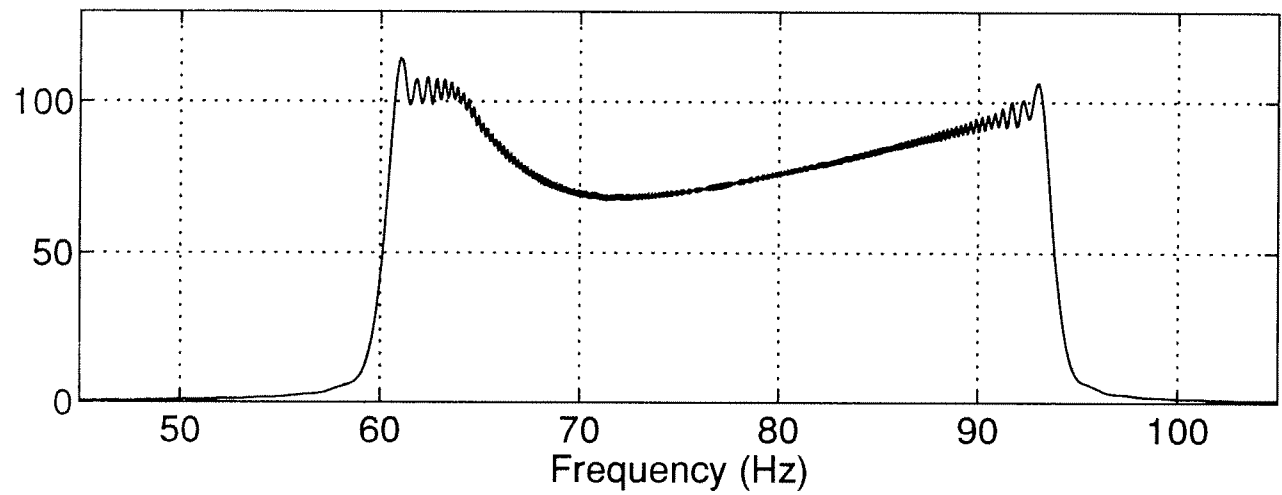
Fig.5b: Phase of AM-LFM spectrum
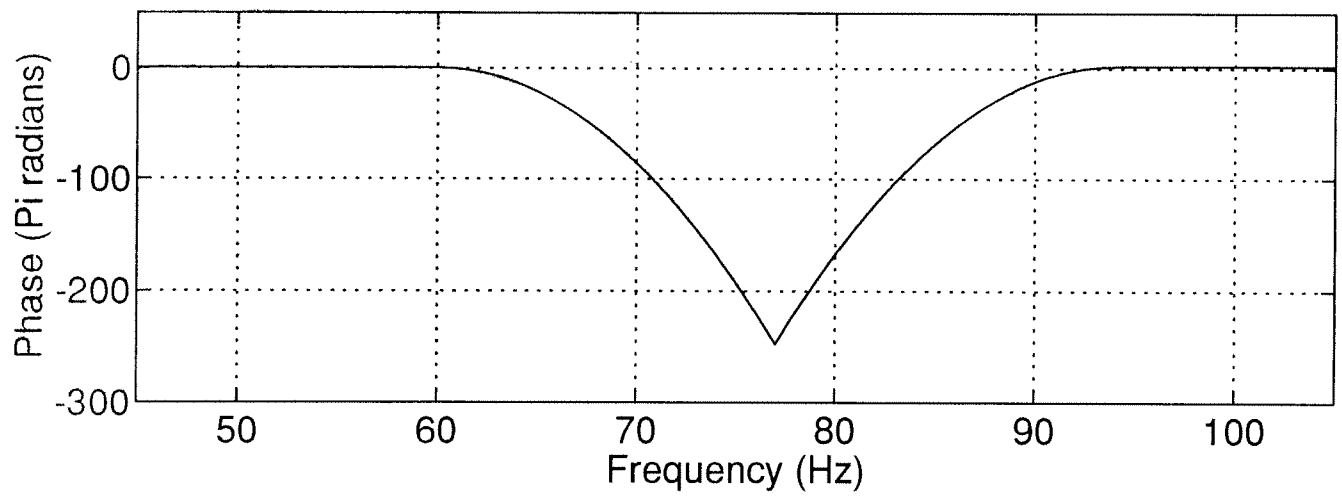
The output sound pressure spectrum is obtained from driving the input voltage spectrum through the linear system (cable 50 n. miles, tuner, transducer 1000 m depth). The squared magnitude of the sound pressure spectrum, known as the output power spectrum, is shown in Figure 6a. The phase of the sound pressure spectrum is shown in Figure 6b. Unfortunately, the output power spectrum does not have a desirable shape. The corresponding autocorrelation function, not shown, would have high time-domain sidelobes.

Fig.6a: Output power spectrum, driven with AM-LFM

Fig.6b: Phase of output pressure spectrum, driven with AM-LFM
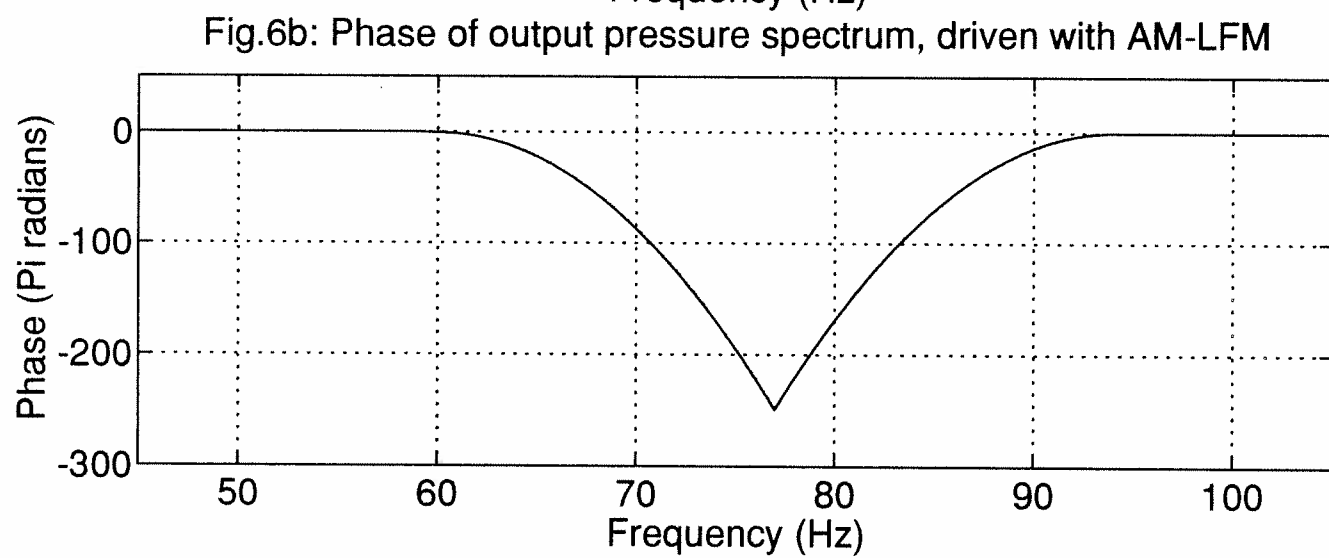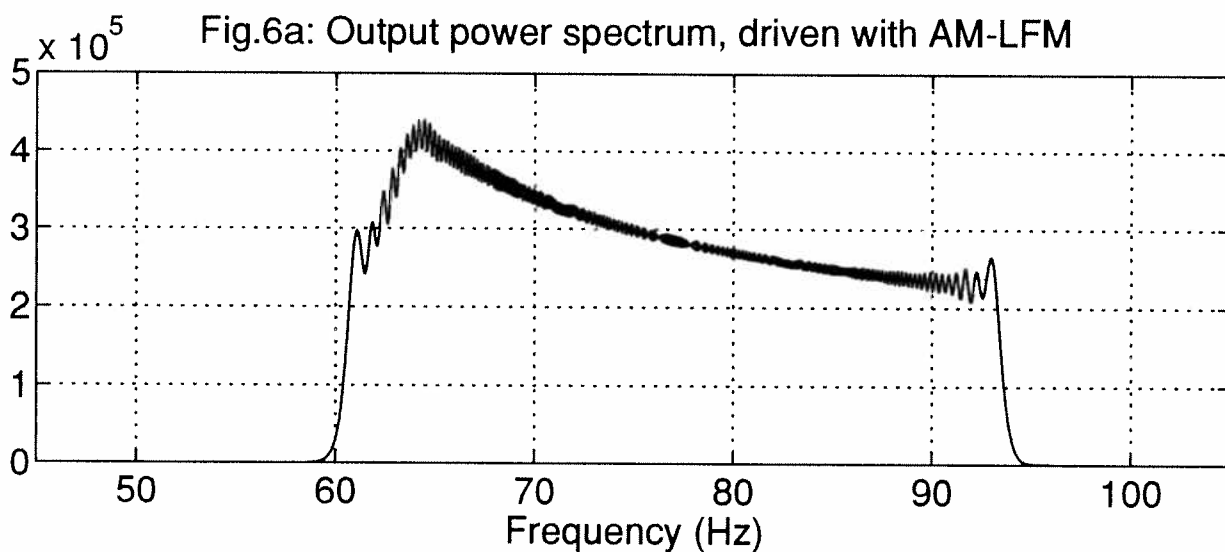
The cable, tuner and transducer were driven with a linear frequency modulated waveform which was also amplitude modulated so that maximum instantaneous power was transmitted. Since the power spectrum of Figure 6 is not of the desired raised-cosine shape, a nonlinear-FM waveform is required to shape the spectrum by "dwelling" at some frequencies longer than others to customize the shape of the power spectrum. Formally, the relative dwell time at each frequency is a derivative, dt/df. The appropriate value is proportional to the desired power spectrum divided by the linear frequency modulated power spectrum of Figure 6.

A raised-cosine power spectrum is selected as the desired power spectrum. The raised-cosine power spectrum has a corresponding autocorrelation function with a narrow main lobe and low time-domain sidelobes. The linear frequency modulated power spectrum of Figure 6 and the desired raised cosine power spectrum are shown together in Figure 7.

The nonlinear frequency modulation is defined by an instantaneous phase argument. This phase argument is ultimately derived from the "time x power = energy" relation, $(dt/df)|P_1(f)|^2 = k|D(f)|^2$. This relation is solved to compute the time corresponding to a given instantaneous frequency, $t(f_{inst})$. The constant k is adjusted to get the desired period T. Integrate to solve the relation

$$t(f_{inst}) = k \int_{f_L}^{f_{inst}} |D(\sigma)|^2/|P_1(\sigma)|^2 d\sigma$$

The power ratio, $|D(\sigma)|^2/|P_1(\sigma)|^2$, is the desired power spectrum divided by the linear frequency modulated power spectrum and is proportional to dt/df. The power ratio is shown in Figure 8. The procedure proceeds to obtain the instantaneous phase argument which will define the nonlinear frequency modulation.

16

Fig.7: Desired and actual output power spectra

Fig.8: dt/df = desired/actual
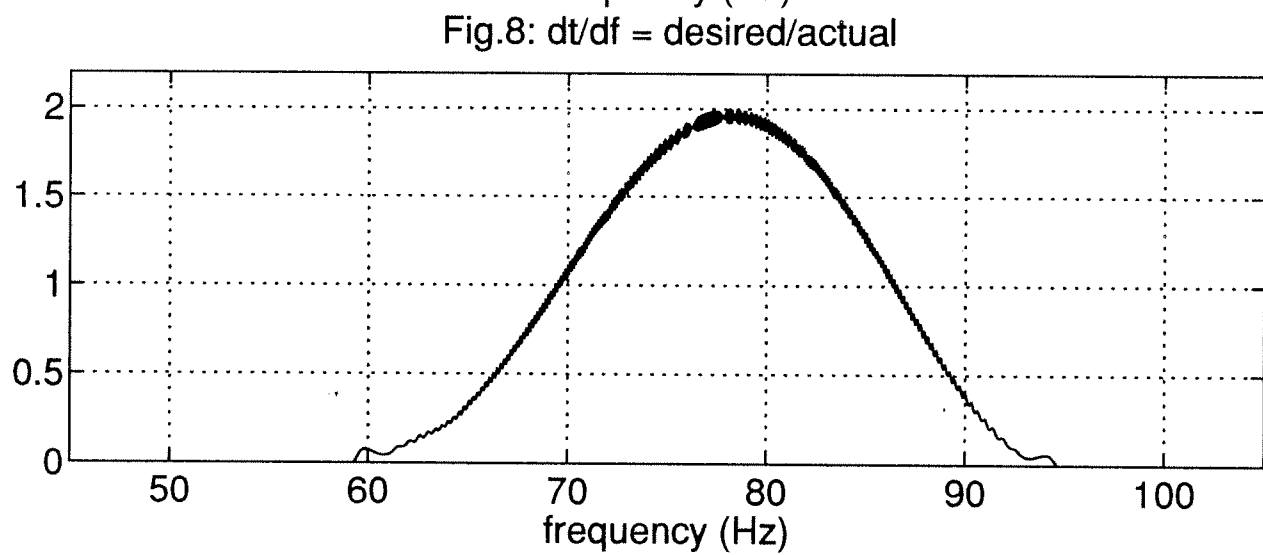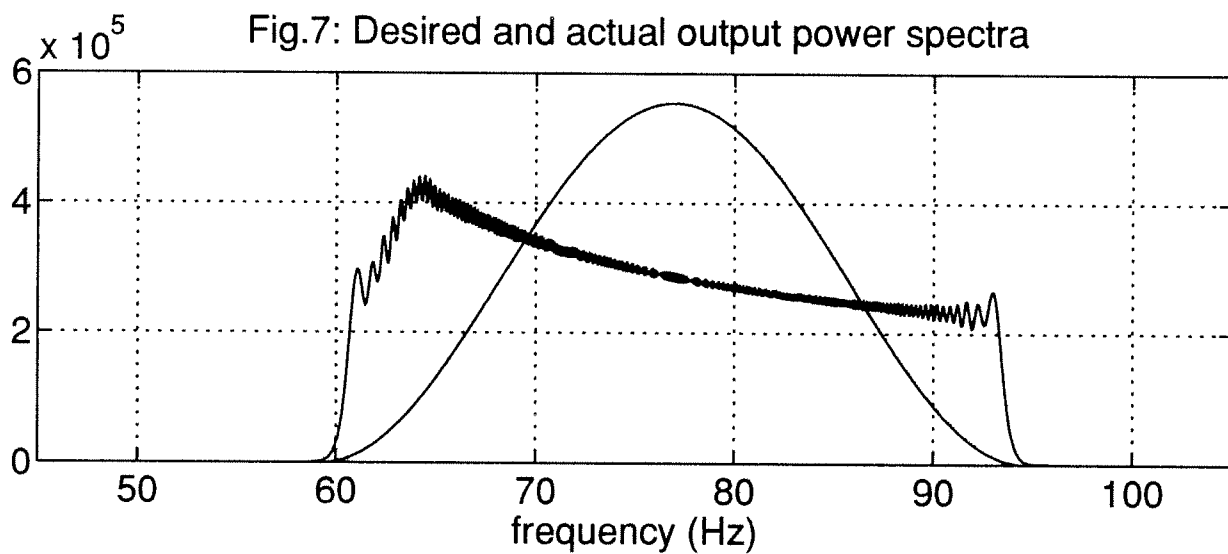
The time the instantaneous frequency is transmitted to define the non-linear frequency modulation, $t(f_{inst})$ is shown in Figure 9. A linear chirp would be a straight line. The function is inverted using numerical interpolation to obtain instantaneous frequency as a function of time, $f_{inst}(t)$, and is shown in Figure 10. The phase as a function of time is obtained by integrating $f_{inst}(t)$

$$\theta_{inst}(t) = 2\pi \int_0^t f_{inst}(\tau)d\tau$$

Fig.9: t(f): time as a function of instantaneous frequency
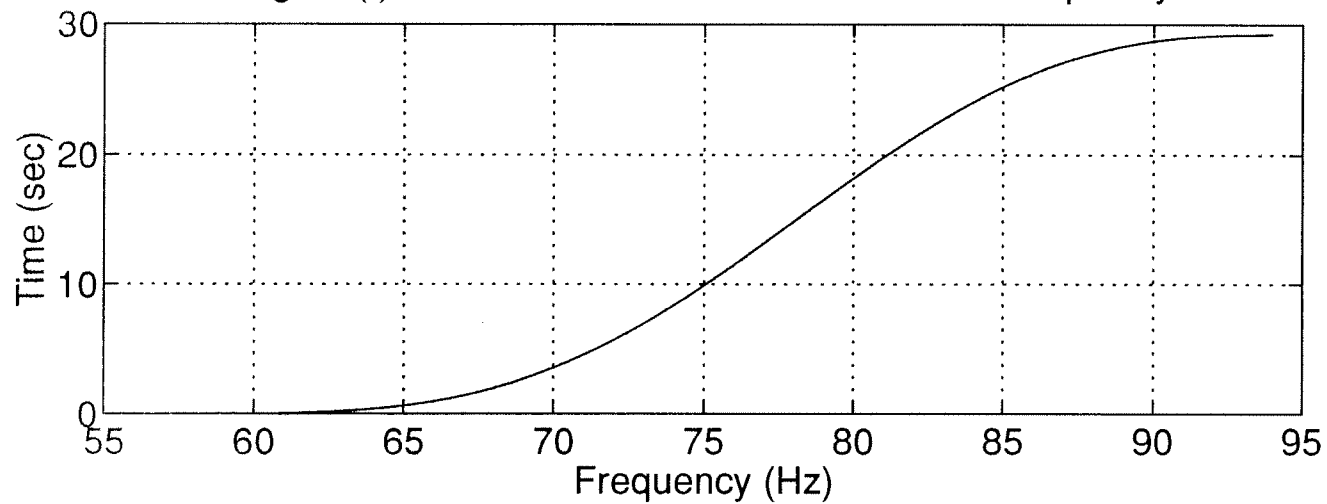
Fig.10: f(t): instantaneous frequency as a function of time
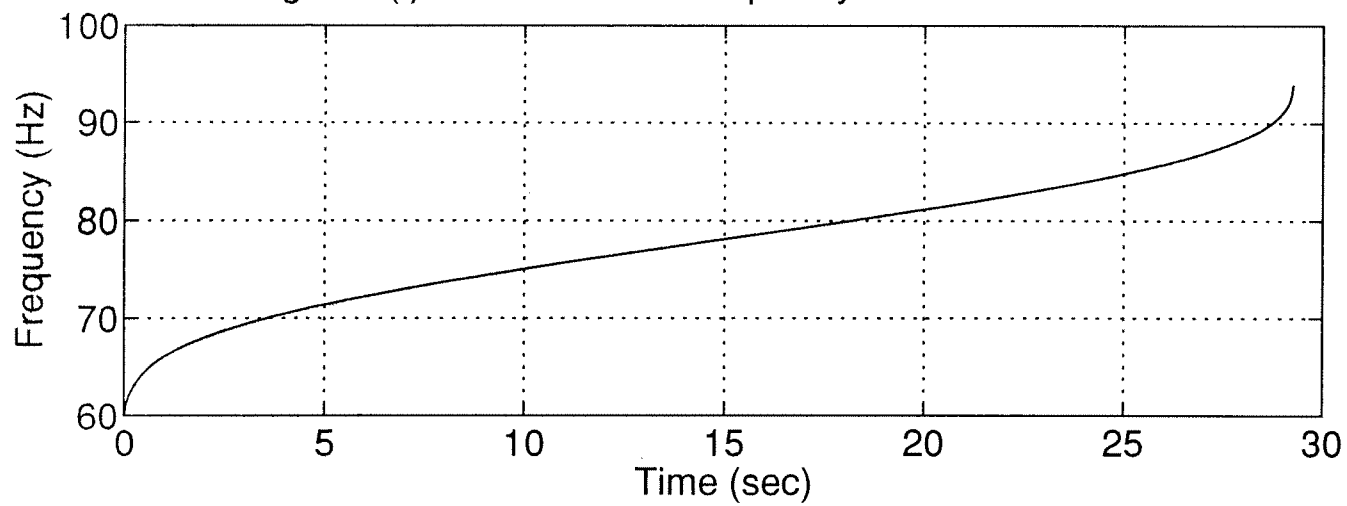
Now that the amplitude (Figure 3) and phase, $\theta_{inst}(t)$, of the input waveform are specified, the input driving voltage waveform is specified.

$$s_3(t) = B(f_{inst}(t))cos(\theta_{inst}(t))$$

This non-linear frequency modulated, amplitude modulated time-domain voltage waveform is shown in Figure 11. The magnitude spectrum of the AM nonlinear-FM input voltage waveform, $s_3(t)$, is shown in Figure 12. A 8192-point Fourier Transform of $s_3(t)$ was used. The magnitude spectrum has a ripple across the band. This ripple will be apparent at the output spectrum as well causing a deviation from the desired magnitude spectrum. First, this error will be viewed, then a procedure to correct this error will be described.

Fig.11: AM-NLFM (baseband)
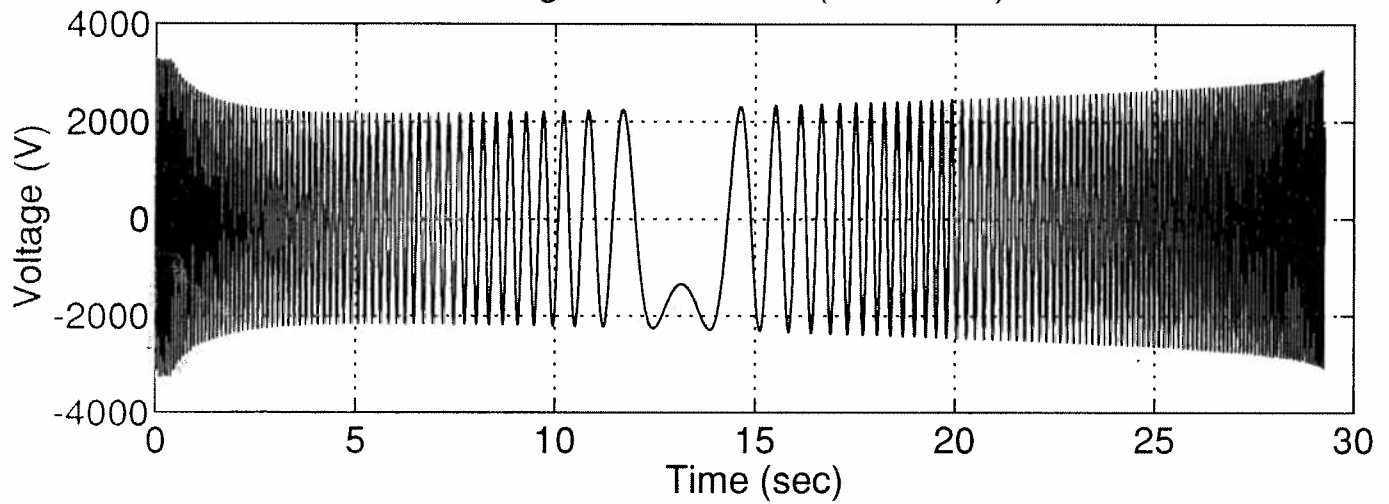
Fig.12: Spectrum of AM-NLFM input signal, with ripples
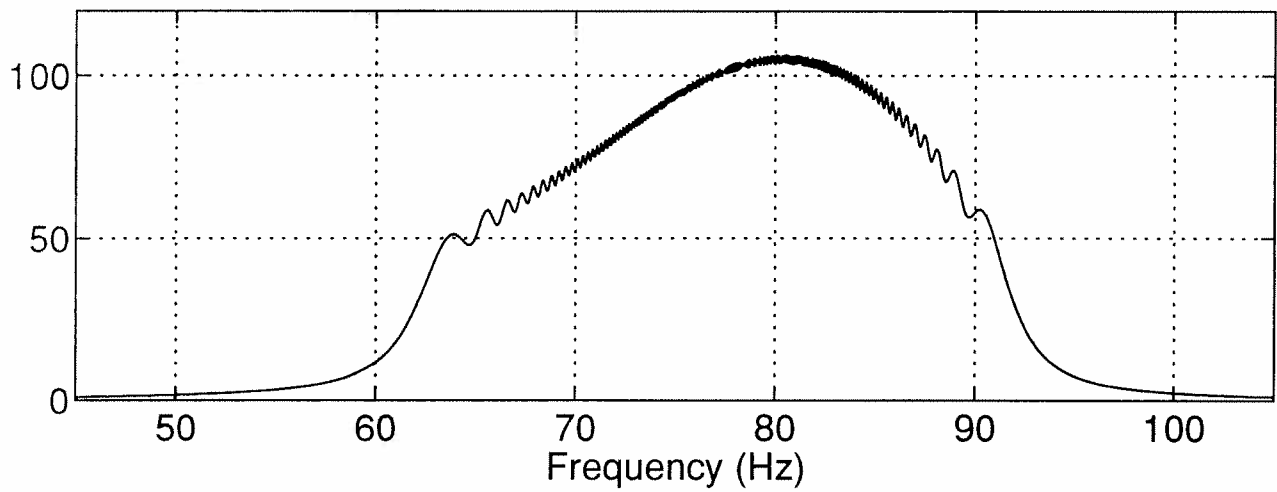
The output power spectrum is calculated using the ABCD matrix description of the linear system and the input voltage spectrum of Figure 11 as an input. The output power spectrum is shown in Figures 13. This power spectrum was designed to have a raised-cosine shape. Figure 14 shows a difference error plot of the designed and desired power spectra. Notice the error energy is spread rather evenly across the band and has a standard deviation of 10010. The error is a "ripple". It is about $1/60^{th}$ of the maximum output power spectrum.

Since the design procedure is meant to drive the transducer as hard as possible, the total output energy is essentially decided by the hardware property (B(f) and H(f)). Choosing different desired output power spectral shapes only slightly affects the total output energy, as shown below here.

spectral shape	total power	(average) SPL
rectangle	2.6206e+8	201.174
triangle	2.8518e+8	201.541
sinc (main lobe)	2.8566e+8	201.548
$\cos^2$	2.8754e+8	201.574
$\cos^4$	2.8708e+8	201.570
$\cos^{16}$	2.8556e+8	201.547

$\times 10^5$ Fig.13: Output power spectrum, driven with rippled AM-NLFM

Total power: 2.875e+08
Dashed: desired shape

Frequency (Hz)

$\times 10^4$ Fig.14: Error=output-desired, with ripples in spectrum

Std=1.001e+04
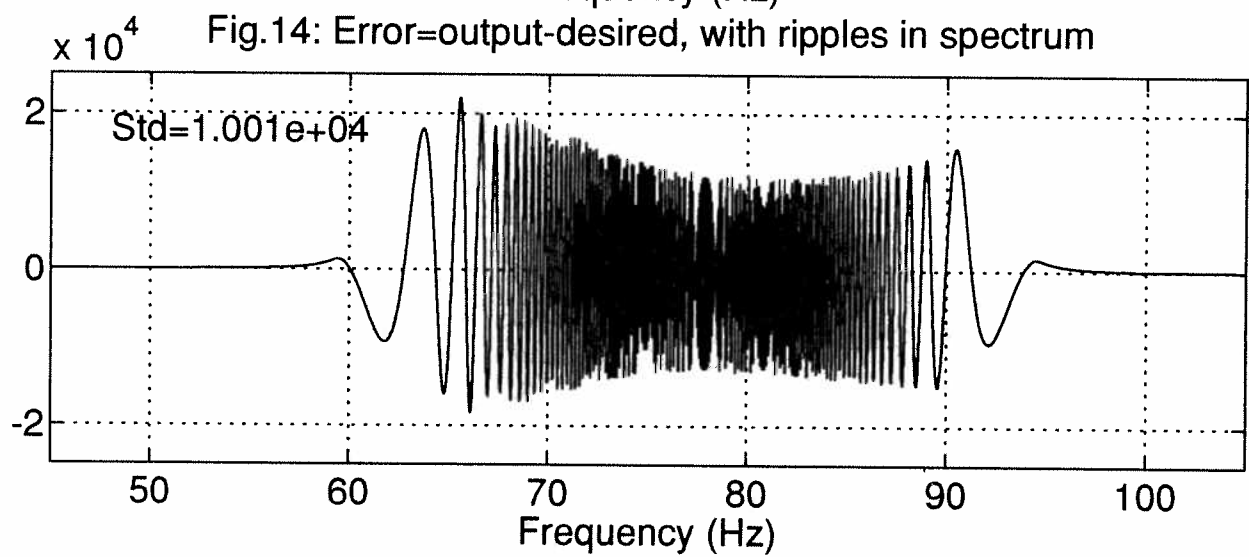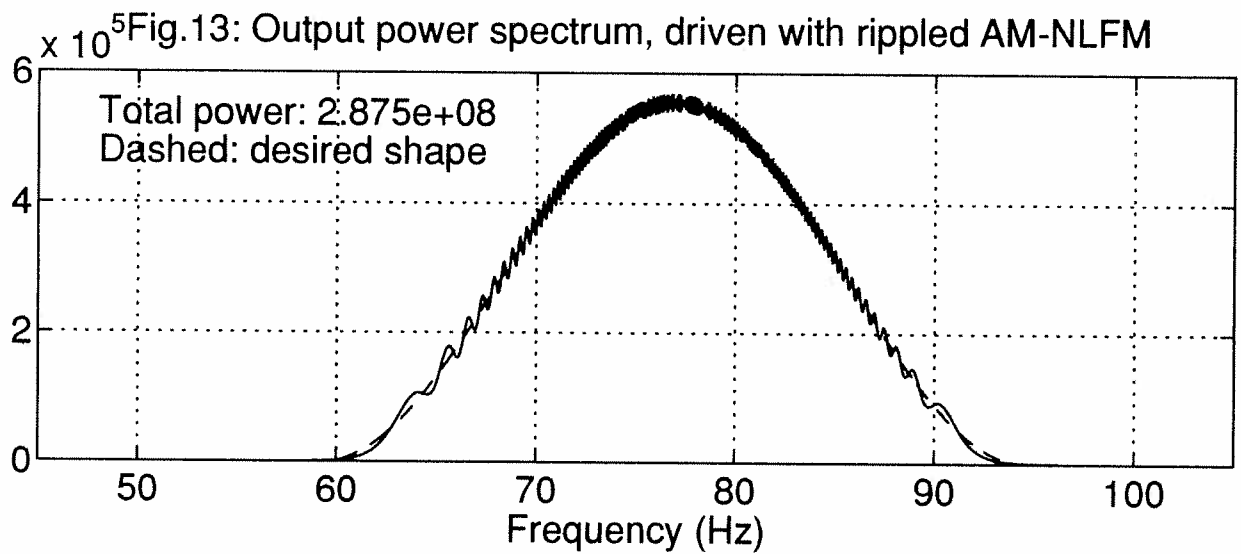
Frequency (Hz)

Figure 15 shows the output sound pressure time-domain waveform. A 8192-point Fourier Transform of the output sound pressure spectrum was used to compute the time-domain sound pressure waveform. Figure 16 shows the phase in the frequency domain for the sound pressure waveform.

It is desired to remove the ripples from the output power spectrum. First, the procedure used to accomplish this will be defined. Second, the methodology behind the approach is described. The spectrum of a new output sound pressure waveform, $P_1(f)$, is constructed using the computed phase of the rippled output pressure spectrum (Figure 16) and a square-root raised-cosine magnitude, the desired shape for this example.

$$P_1(f) = \sqrt{raised\quad cosine(f)} \quad cos(phase(f))$$

This spectrum has exactly a desired shape. Therefore, the matched filter output, the Fourier transform of the power spectrum, will be that of the desired waveform. The corresponding time-domain waveform is $p_1(t)$.

x 10^4   Fig.15: Output pressure (baseband), with spectral ripples
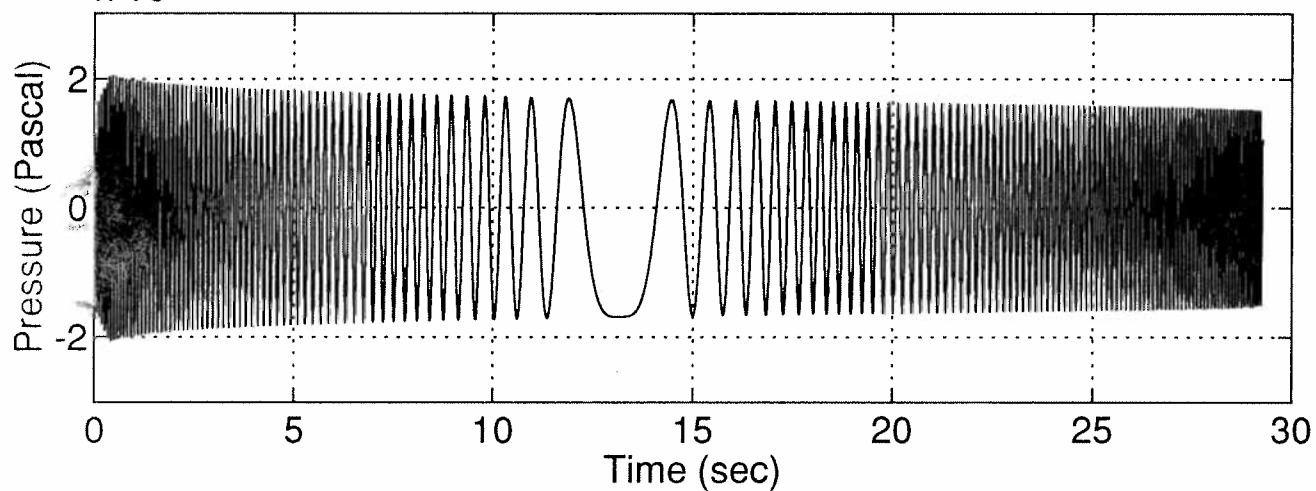
Fig.16: Phase of rippled output pressure spectrum
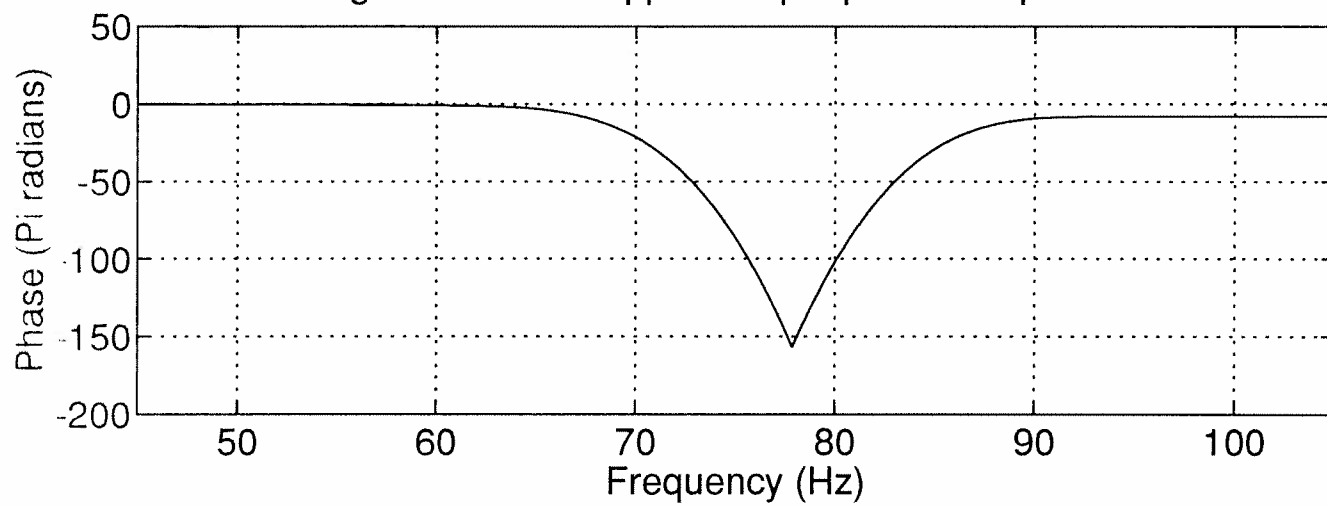
The de-rippled Spectrum, $P_1(f)$, is passed backward through the linear system to derive the corresponding input voltage spectrum. This input voltage spectrum is transformed into the time-domain and this de-rippled input voltage waveform is shown in Figure 17. The new input voltage waveform must be checked to assure that this maximum allowable input voltage, as shown by the dashed curve in this figure, is not surpassed. Unfortunately, in this case, this constraint is overshot at the beginning and end of the chirp period.

It is seen from Figure 17 that the removal of spectral ripples introduces ripples in the envelope of the time-domain waveform. These time-domain ripples cause overshooting at the beginning and the end of the chirp period. The cable voltage limitation is violated in this case. In order to remedy this problem, it is necessary to modify the input voltage waveform. There are two ways of achieving this. One is to level the input voltage level at this point, causing a departure of the signal from the desired waveform, and therefore, a degradation in matched filter performance. The other is to modify B(f) so that the instantaneous amplitude rises and falls gradually, avoiding overshooting of the input voltage. The second method is preferable because it does not degrade the output power spectral shape, and the reduction of transmitted instantaneous power is comparable to the first method.

With modified B(f) shown in Figure 18, a new AM nonlinear-FM signal can be formed using the above described procedure.

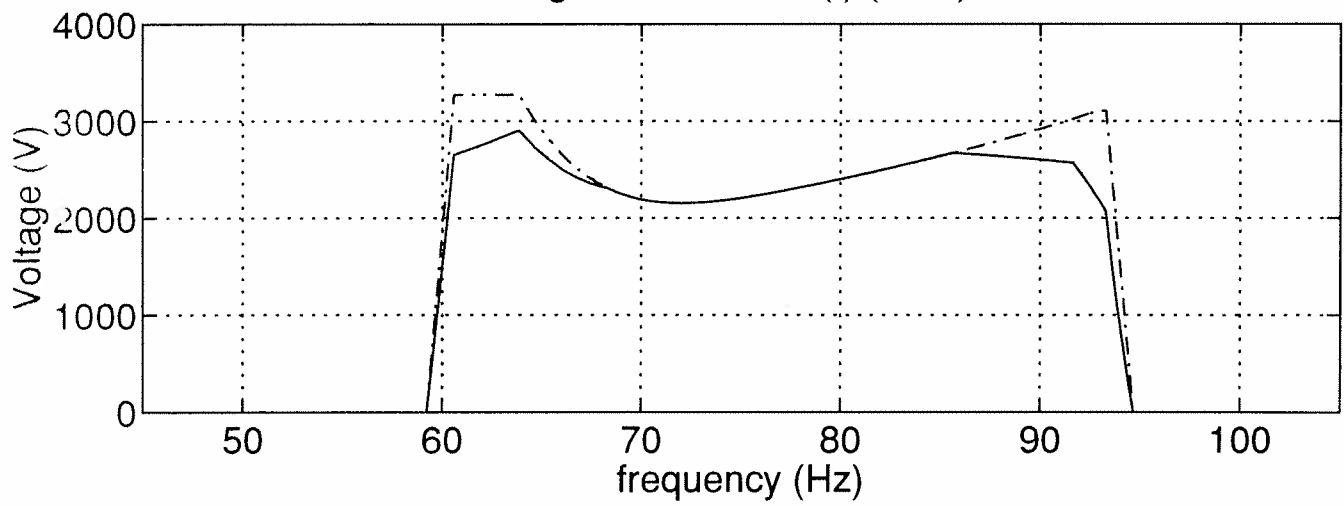Fig.17: De-rippled input waveform, with overshooting
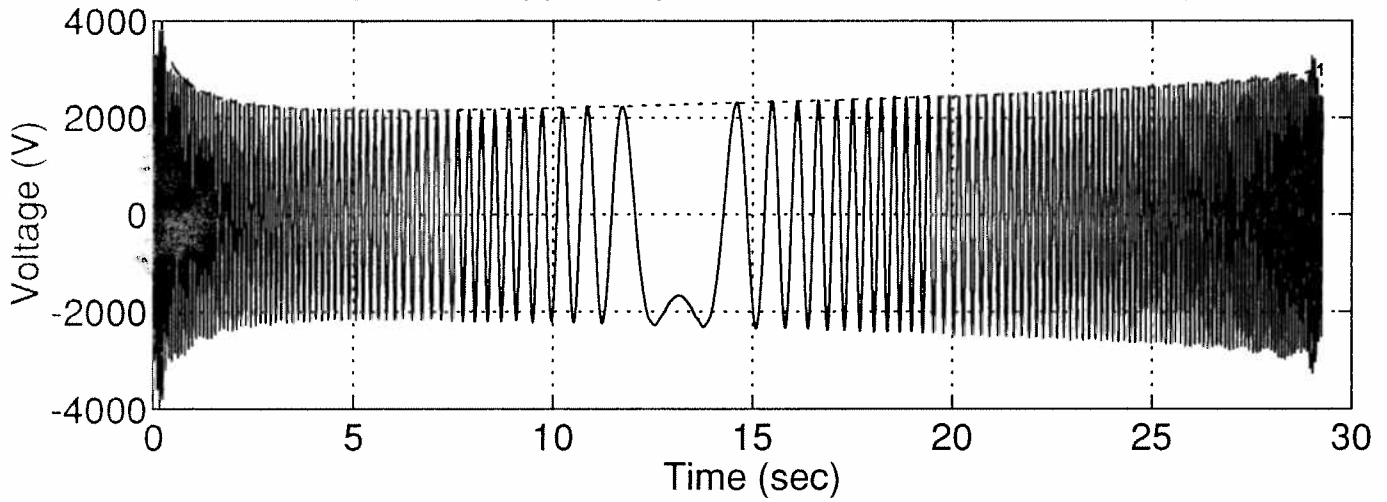
Fig.18: Modified B(f) (solid)

The chirped waveform will be periodically repeated. Therefore the "two ends" of the chirp should have a smooth transition in phase. If this is not the case, a spike in the time-domain will result. Figure 19a shows the time-domain waveform of the AM nonlinear-FM input waveform at this transition. Figure 19b shows the phase of the waveform at the transition. By slight extrapolation of $f_{inst}(t)$, this phase mismatch is corrected.

Fig.19a: AM-NLFM at transition of adjacent periods
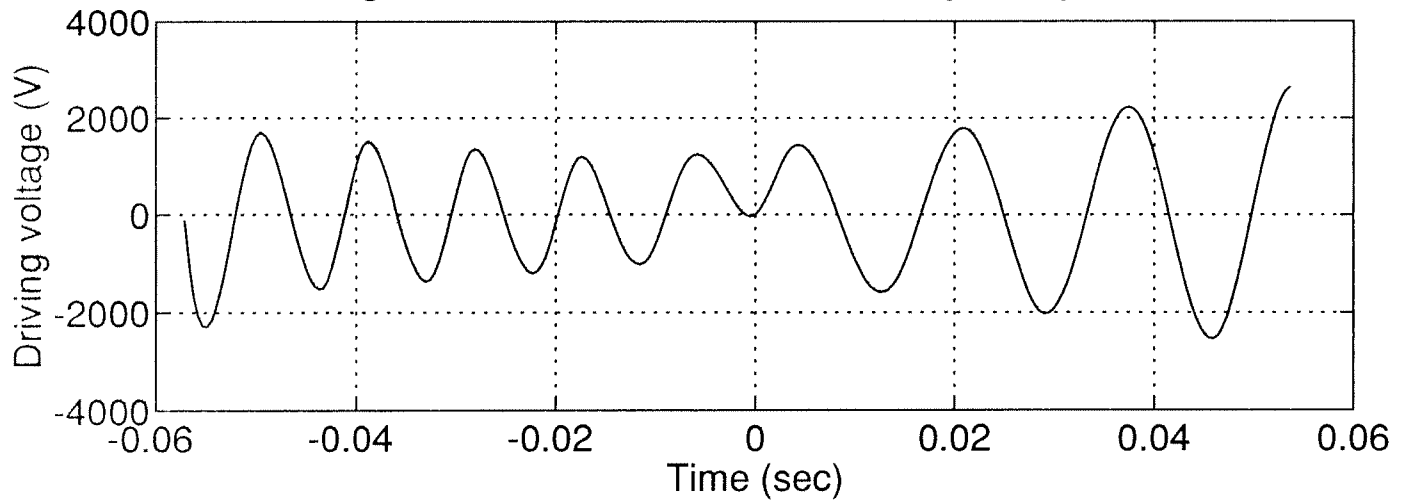
Fig.19b: Phase of AM-NLFM at transition
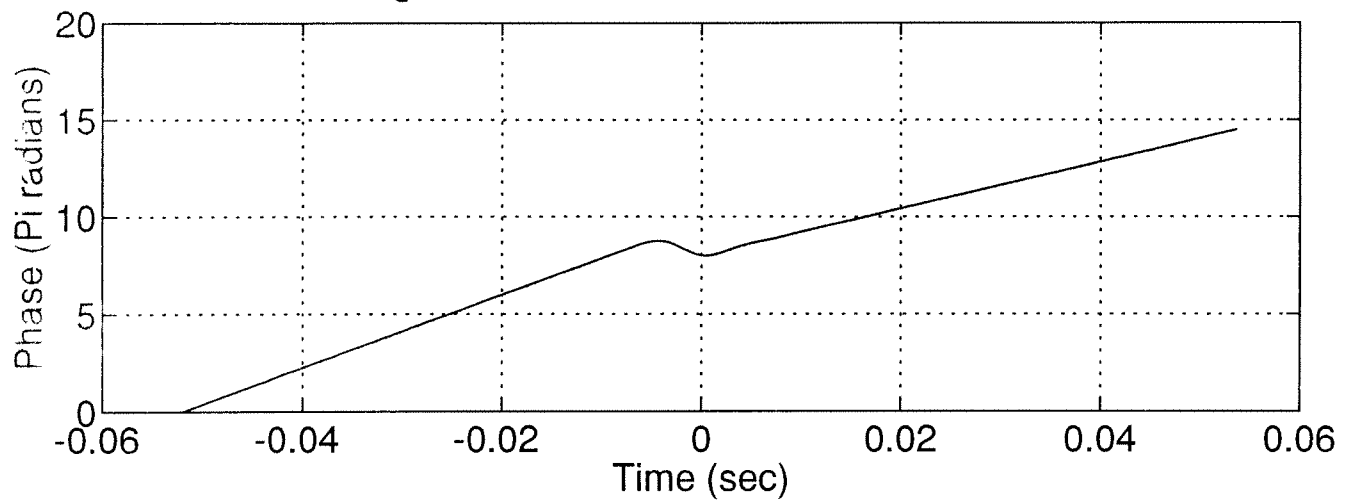
Figure 20a shows the AM nonlinear-FM input waveform resulting from correction of the phase mismatch at the transition. Figure 20b shows the corresponding phase waveform as a function of time at the transition. The change in slope of the phase waveform corresponds to the change in instantaneous frequency from 94 to 60 Hz.

Fig.20a: AM-NLFM, phase matched at transition
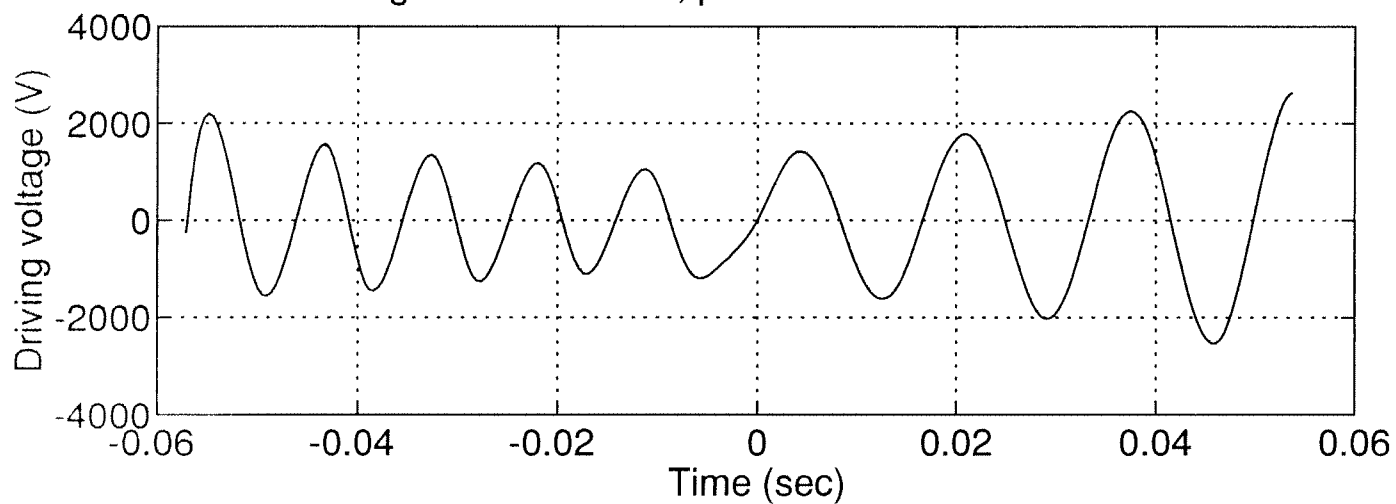
Fig.20b: Phase of AM-NLFM at transition, phase-matched
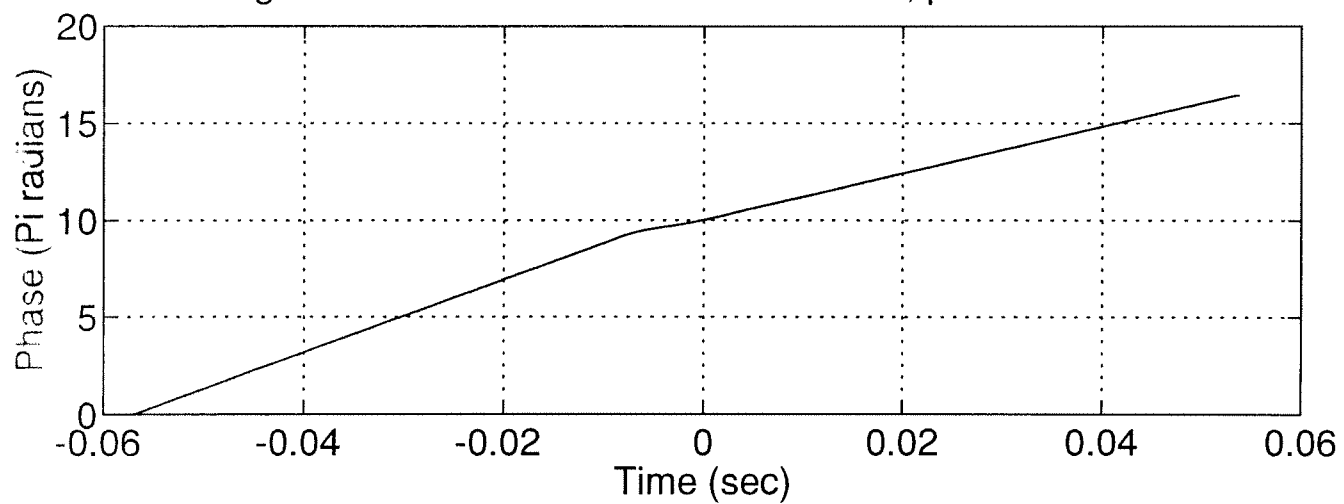
Figure 21 shows the designed input waveform which is within the maximum allowable input voltage. Figure 22 compares the input voltage spectrum magnitude rippled (dashed) and de-rippled (solid) cases. The ripples have been removed from the input spectrum so there is reason to expect the spectral ripples will be removed at the output.

Fig.21: The designed input waveform
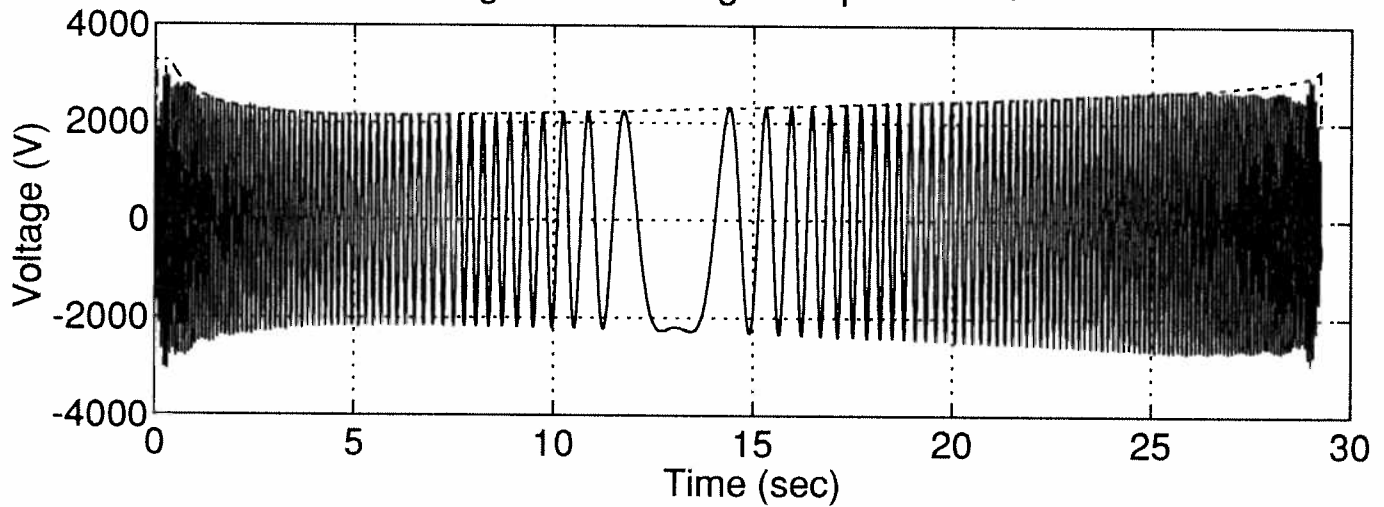
Fig.22: The designed input spectrum

Solid: designed(de-rippled)
Dashed: rippled
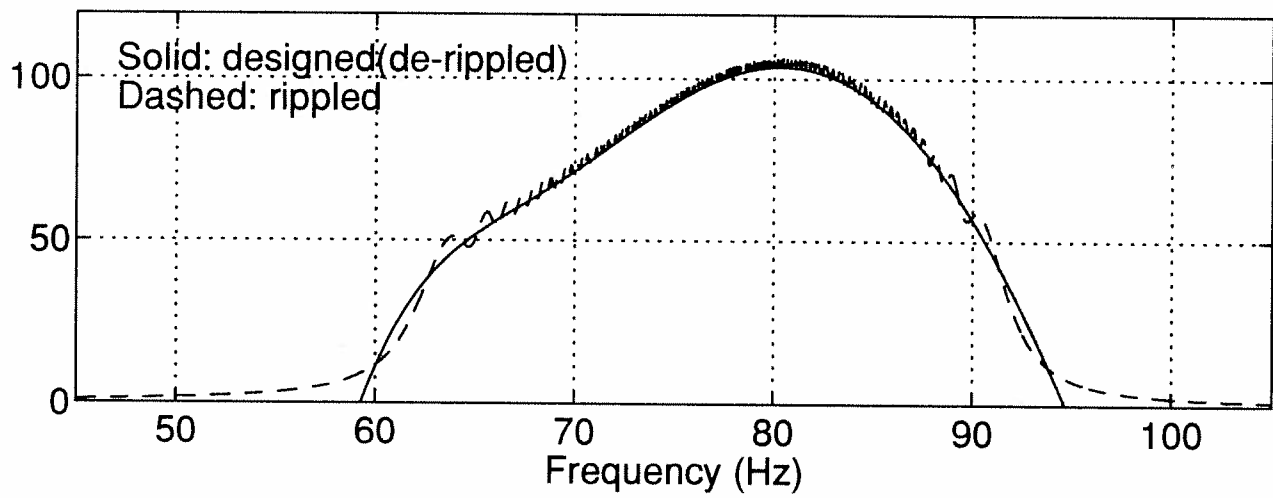
The output power spectrum is computed from the input voltage spectrum and the ABCD matrix of the system. Figure 23 shows that in the frequency domain the ripples have been removed, and the power spectrum is exactly the desired raised-cosine shape. The total power noted on the figure reflects a 0.12 dB loss from the total power with the approximate raised-cosine shape. See Figure 13. It will be shown that the matched filter performance for the de-rippled case is significantly superior. The difference error of the actual power spectrum and the desired spectral shape is shown in Figure 24. The error is solely a result from computational round-off error when the spectrum was computed backward then forward through the system (ABCD matrix).

Fig.23: The designed power spectrum

Fig.24: Computational error in the power spectrum
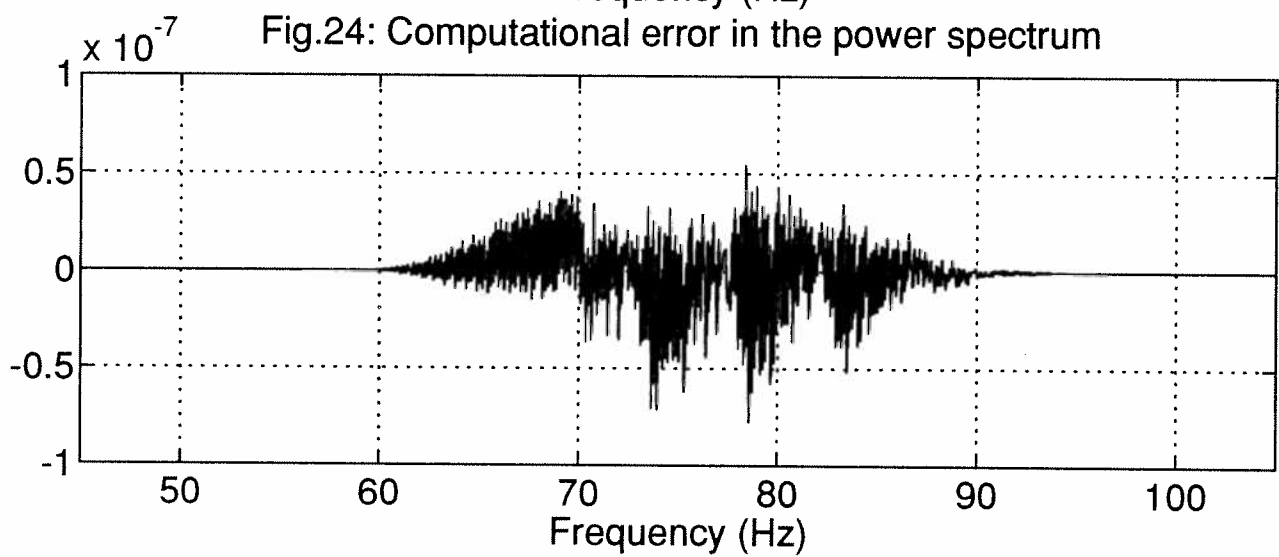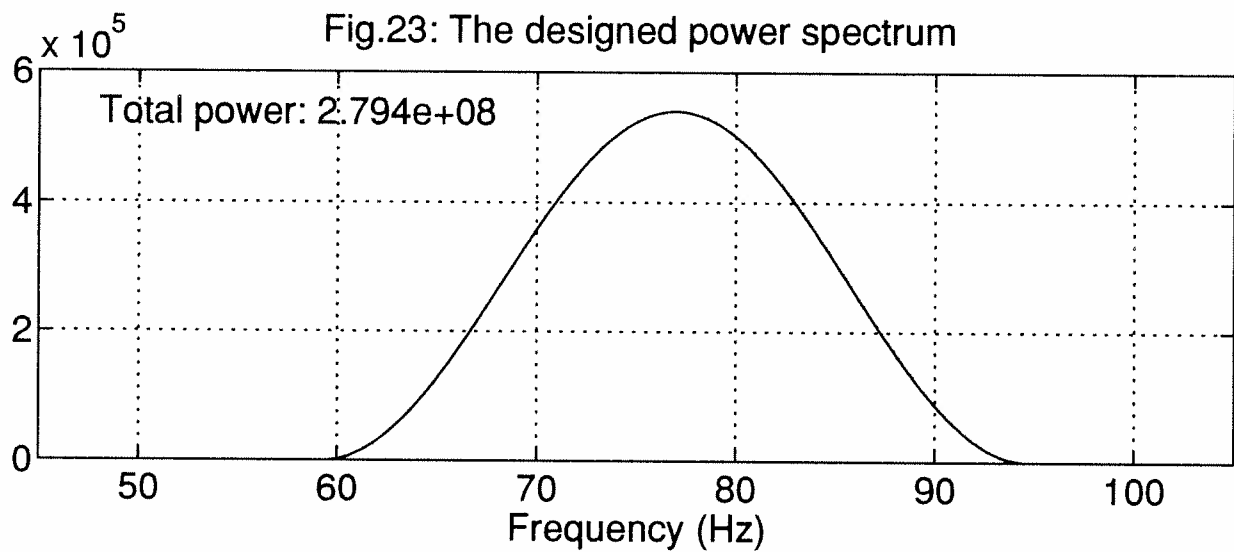
Figure 25 shows the output pressure waveform. Figure 26 shows the rms output sound-pressure level (SPL) as a function of time. The output SPL is approximately flat and consistently exceeds 200 dB referenced to 1 micro Pa measured 1 meter from the source. This was the required specification of the designed transducer.
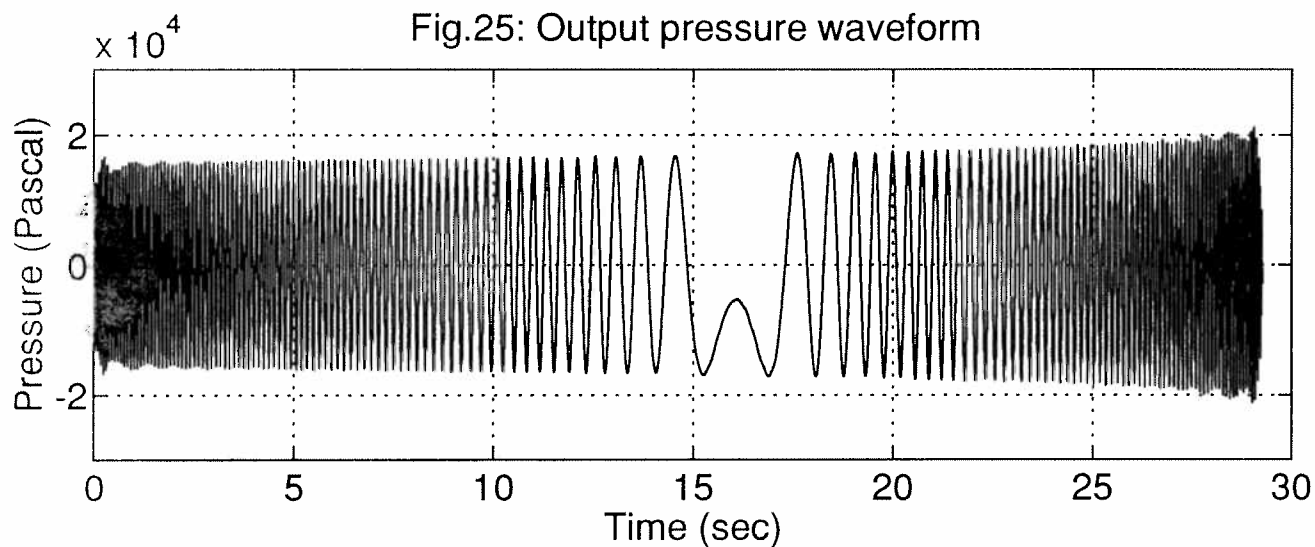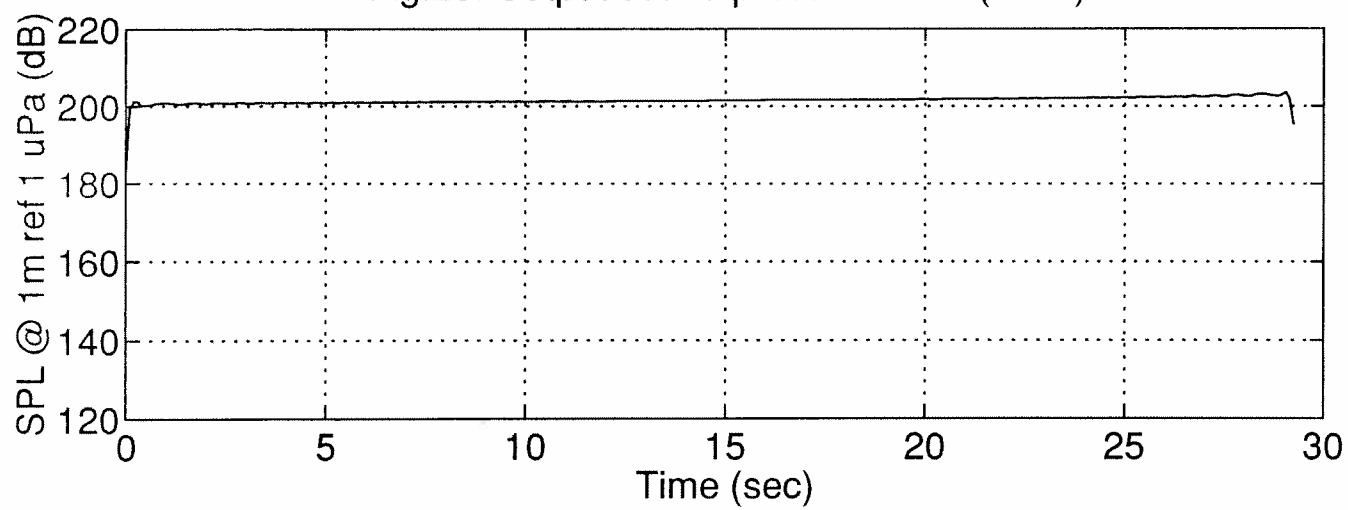
Fig.25: Output pressure waveform

Fig.26: Output sound pressure level (RMS)

The next set of plots investigates the time-domain waveform at critical probe points inside the system. At each point, the waveform is confirmed to not exceed the hardware design specifications. Also, the ceramic stack voltage and stress waveforms will be inspected to validate the quasi-steady-state approximation. The input driving current time-domain waveform is shown in Figure 27a. Figure 27b shows the rms value of the input driving current. The average value is 5.455 amps. The cable is tested to a maximum allowable rms current value of 9.0 amps.

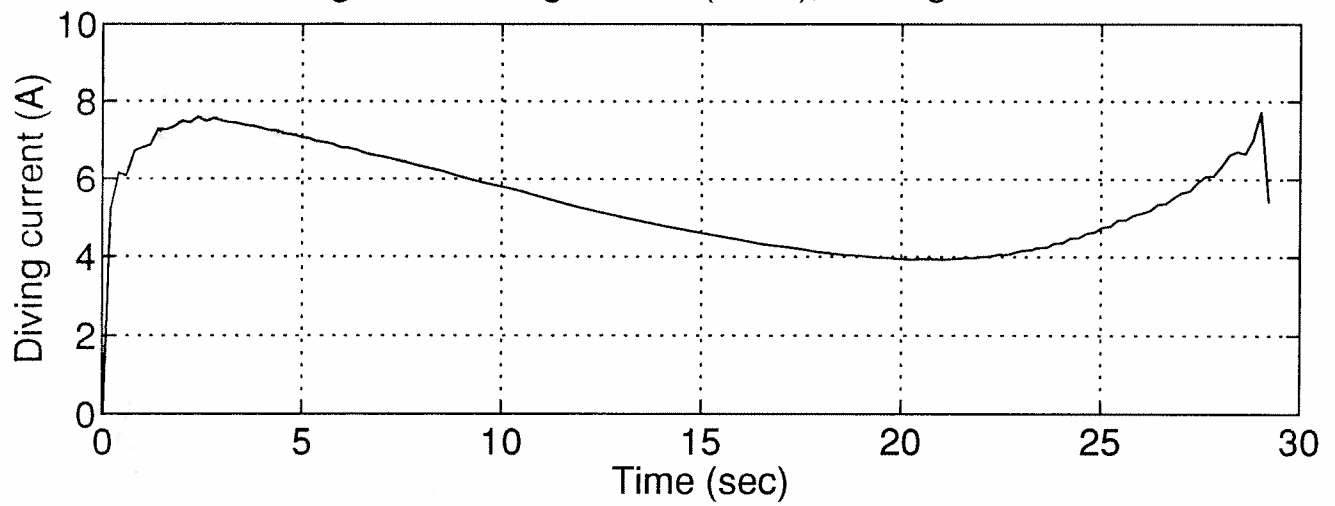Fig.27a: Driving current (baseband): AM-NLFM
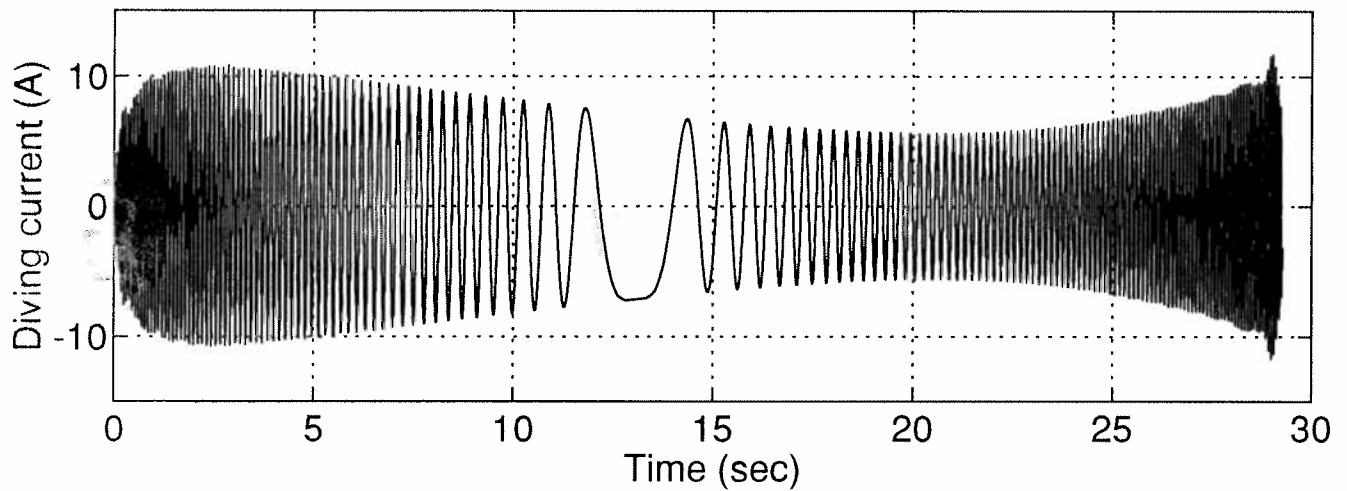
Fig.27b: Driving current (RMS), average=5.455A

The time-domain ceramic stack voltage should not have a peak greater than 5671 volts. (5671 peak = $\sqrt{2}$ x 4010 rms) Figure 28a shows the time-domain voltage waveform. By design, the maximum voltage is met at the beginning and end of the chirp. See Figure 2. The rest of the time, the input driving voltage amplitude is stress constrained. Figure 28b shows the rms voltage across the ceramic stack. This is the envelope of the previous plot divided by $\sqrt{2}$ to convert peak envelope to rms envelope. From this plot it is clearly seen the 4010 volt rms value is not violated. The quasi-steady state design assumption was used to design the input voltage waveform. Since the actual waveform meets the constraints, this is further validation of the quasi-steady state design approach.

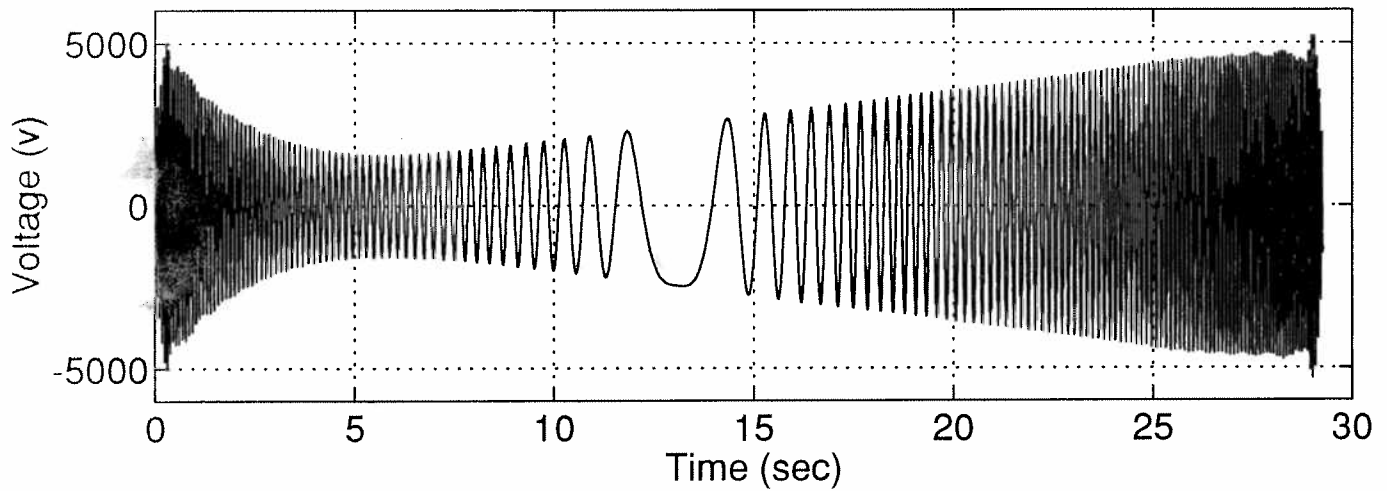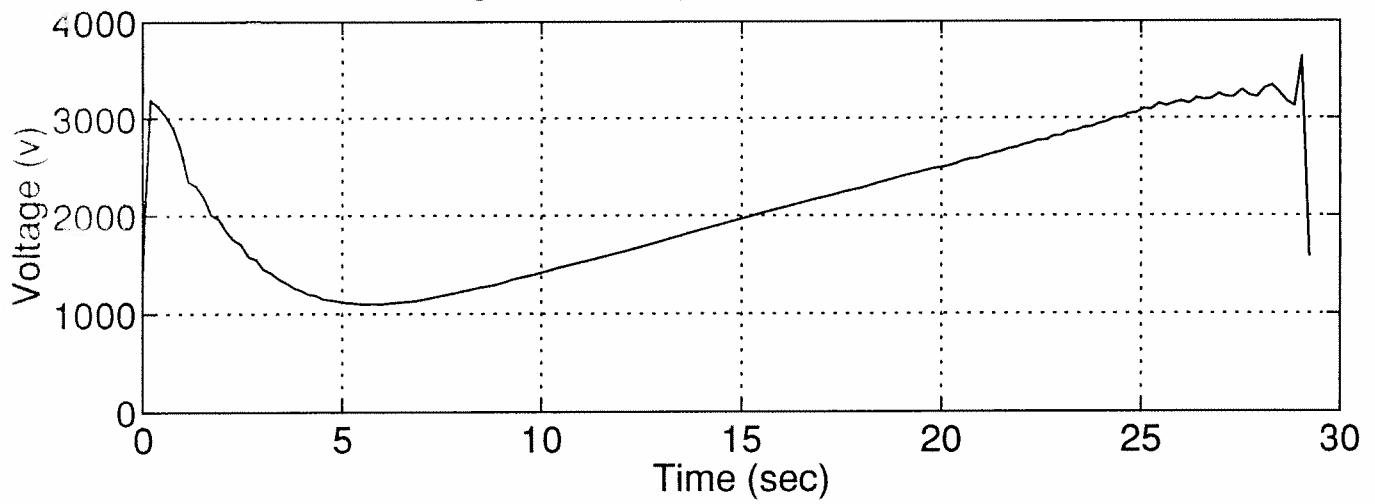Fig.28a: Voltage across stack (baseband)

Fig.28b: Voltage across stack (RMS)

The stress time-domain waveform should not have a peak greater than 3206 psi. The time-domain stress waveform is plotted in Figure 29a. Figure 29b shows the rms value of the stress as a function of time. The constraint is not exceeded. This is the final validation of the quasi-steady-state design approach.
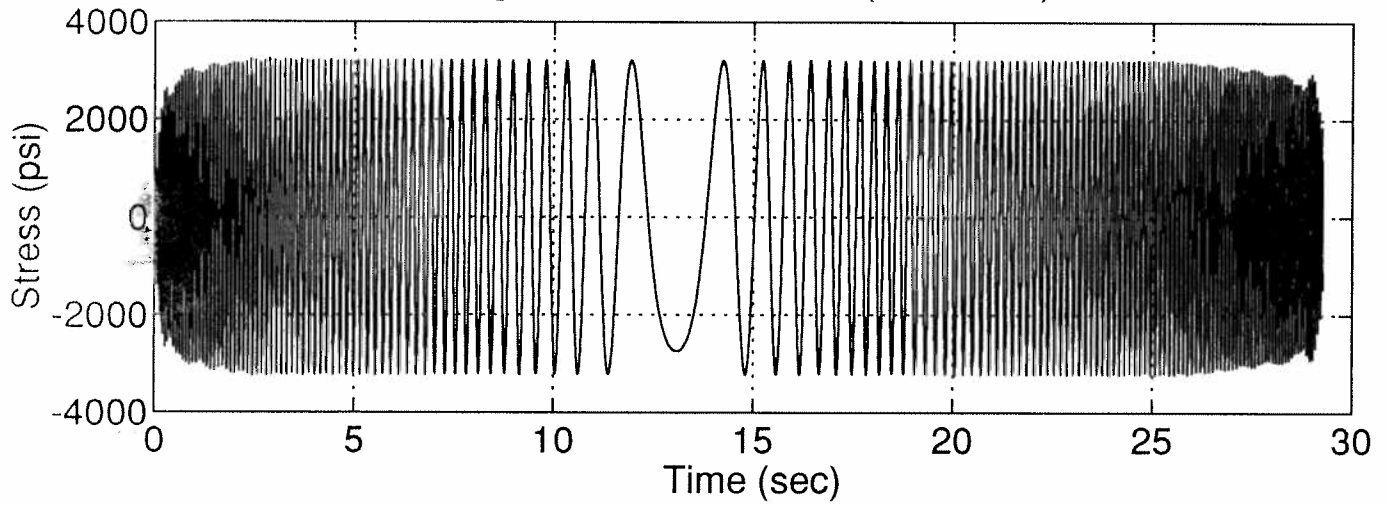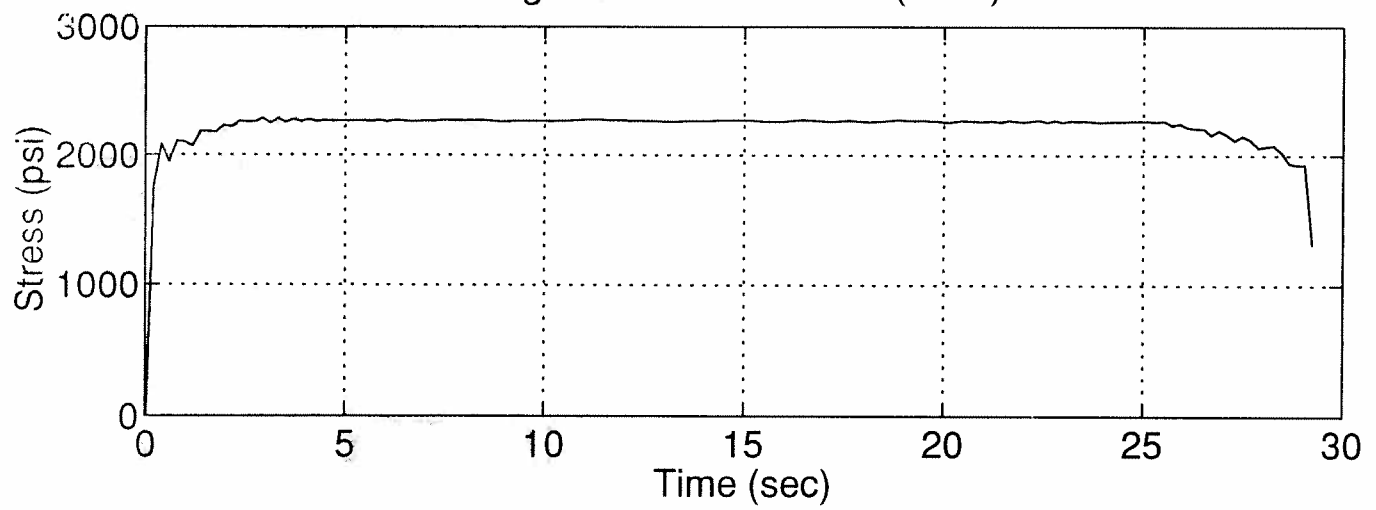
Fig.29a: Stress in stack (baseband)

Fig.29b: Stress in stack (RMS)

The time-domain current waveform into the ceramic stack is shown in Figure 30a. Figure 30b shows the instantaneous rms current into the ceramic stack. The average current is 2.993 amps. The maximum allowable current into the stack is 7.5 amps rms.
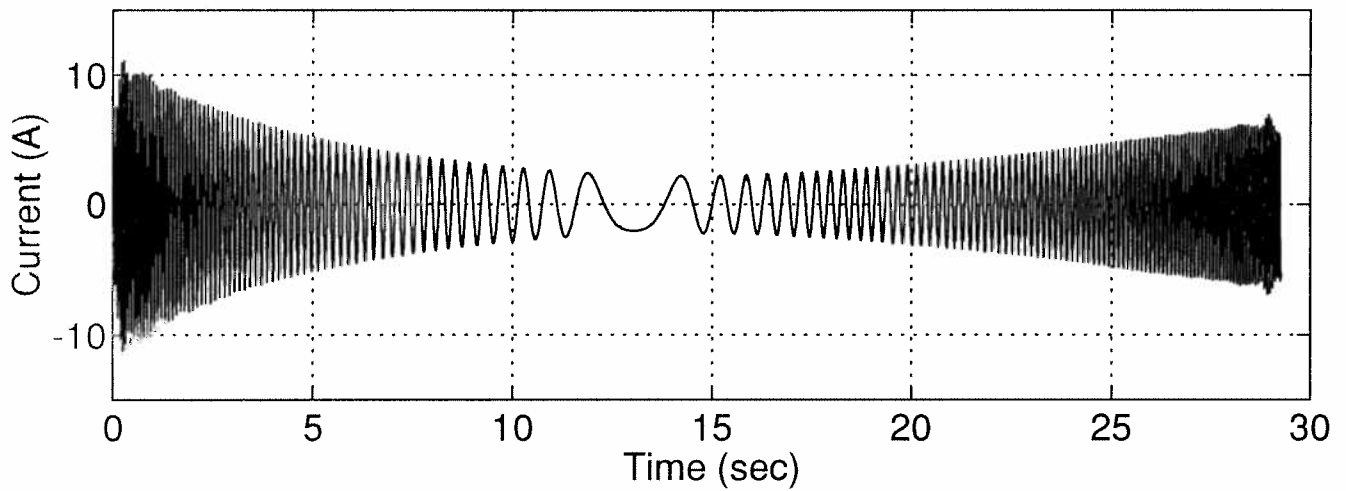
Fig.30a: Current into stack (baseband)

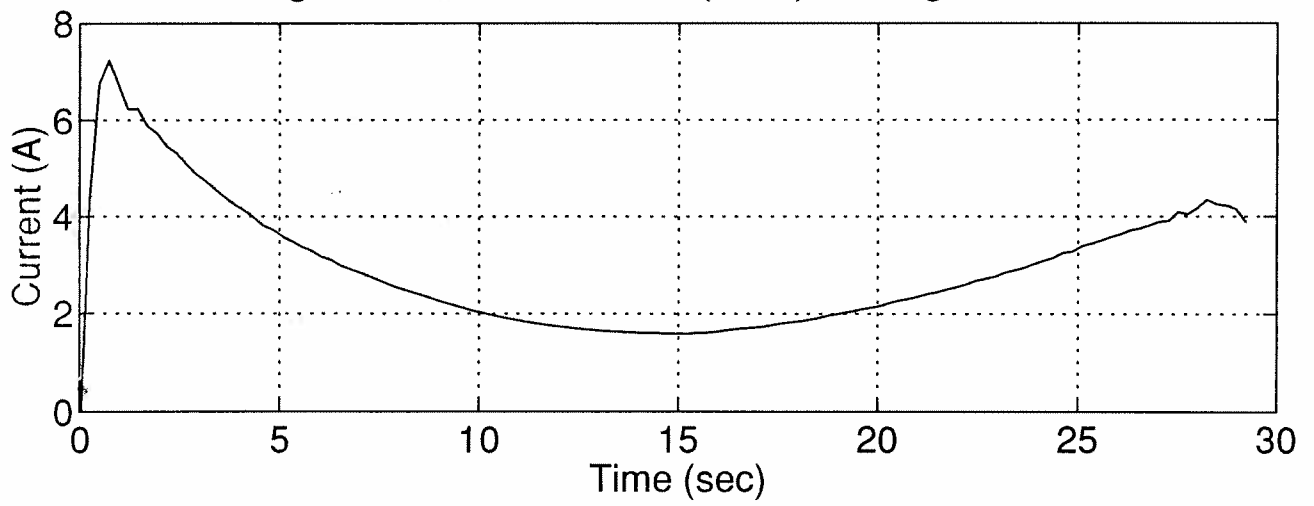Fig.30b: Current into stack(RMS), average=2.963A

Figure 31a shows the time-domain waveform of the current flowing into the tuner. Figure 31b shows the instantaneous rms current flowing into the tuner. The average current value is 6.155 amps. This value is not to exceed 7.4 amps.
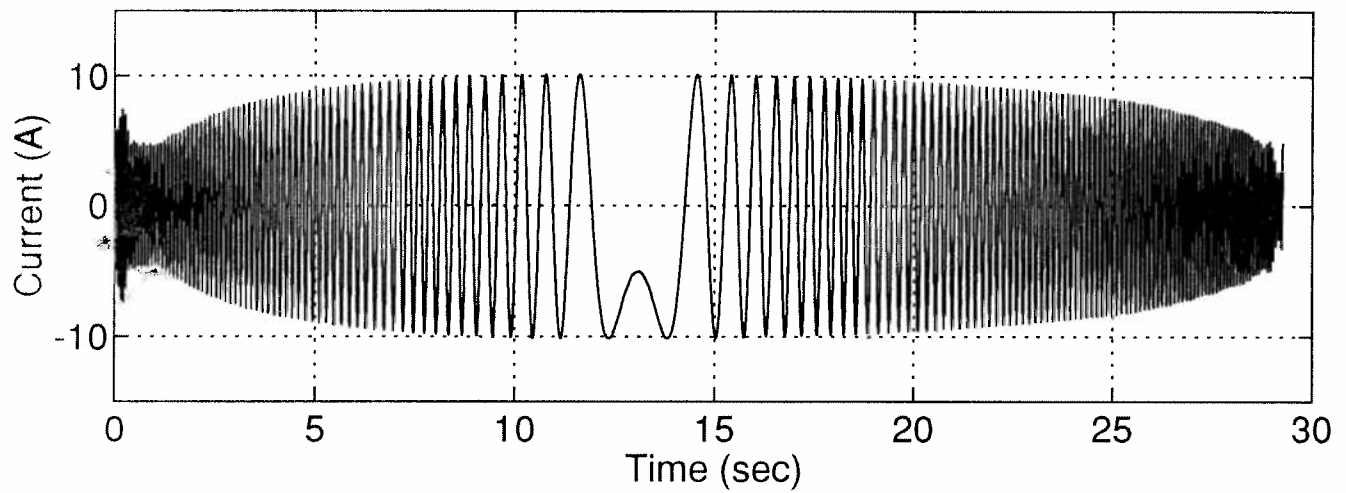
Fig.31a: Current into tuner (baseband)

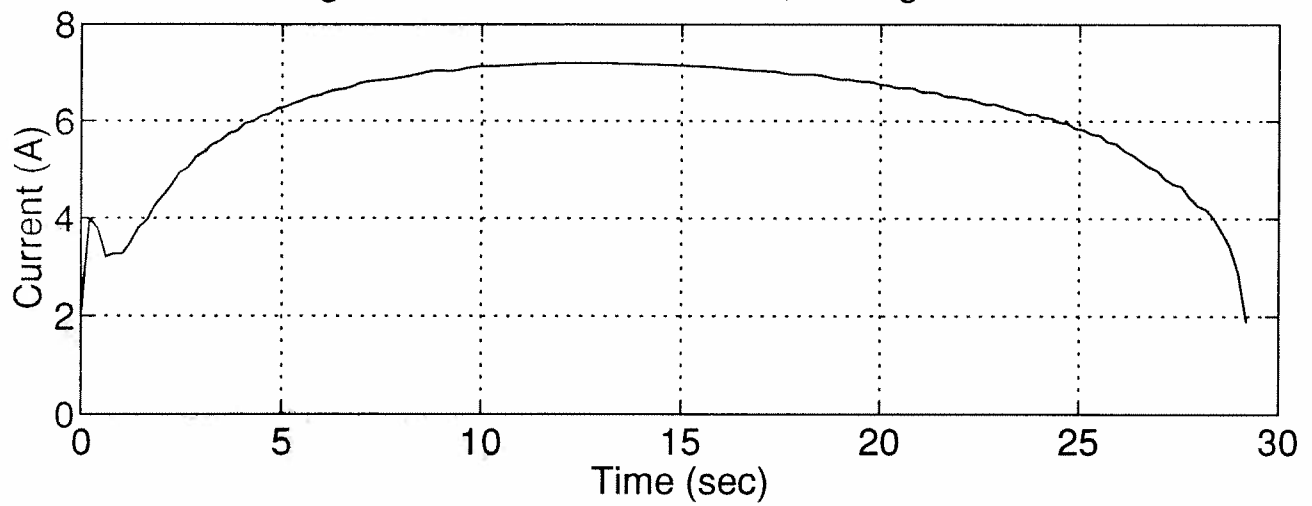Fig.31b: RMS current in tuner, average=6.155A

Figure 32a shows the time-domain waveform of the voltage across the tuner. Figure 32b shows the instantaneous rms voltage across tuner. This voltage is not to exceed 2005.0 volts.

The design method used the quasi-steady state approximation. By checking that the designed waveform has a desired output power spectral shape and does not violate the maximum allowable ceramic stack voltage or stress, the quasi-steady state approximation is validated. Moreover, the current and voltage waveform entering the cable, tuner, and stack were confirmed to be within the allowable specification. Next, the time resolution and signal-to-noise ratio (SNR) properties of the waveform will be investigated.

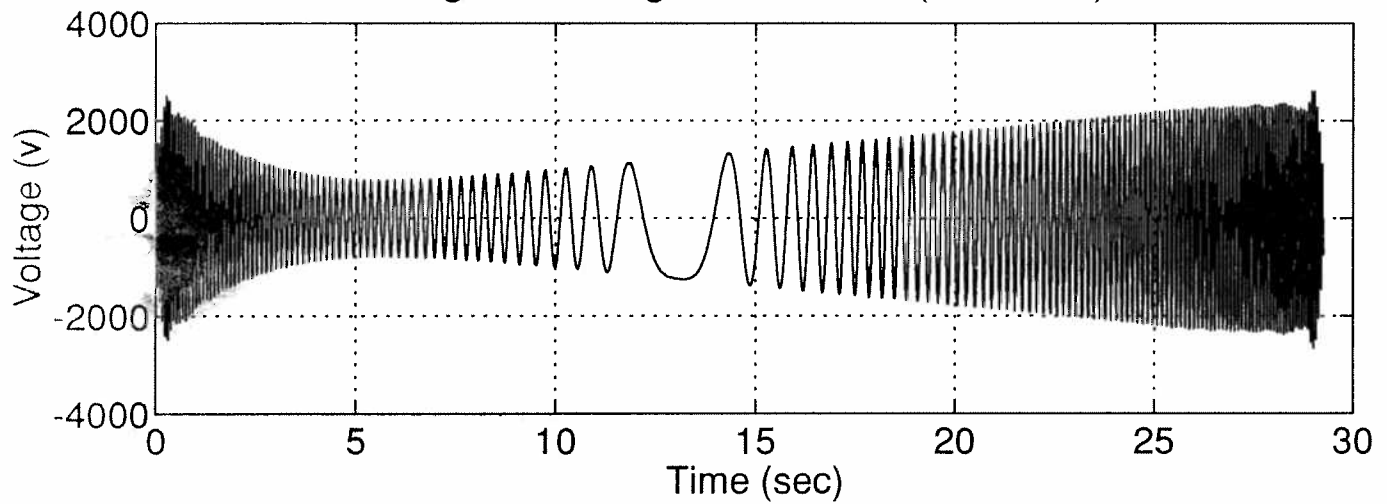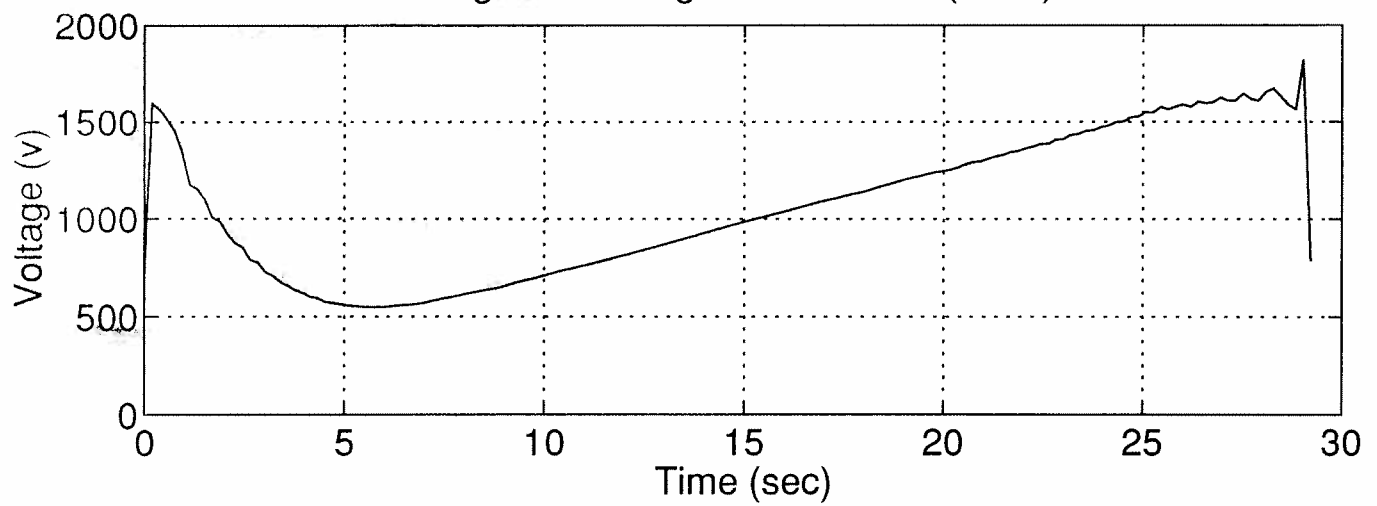Fig.32a: Voltage across tuner (baseband)

Fig.32b: Voltage across tuner (RMS)

The received waveform is processed in two steps. First the received signal is phase-only matched filtered. Roughly speaking, this takes the time distributed energy and compresses it such that all the energy appears to have arrived at nearly the same time. This is how a matched filter processes the spectral phase of the received signal. The output of this phase-only matched filtering will have a higher resolution, but also higher time-domain sidelobes than phase and amplitude matched filtering. Phase and amplitude matched filtering is what is commonly and simply referred to as "matched filtering". Higher time-domain sidelobes implies lower SNR. If a higher SNR is required, additionally, the amplitude of the received signal must be filtered. This is the second part of matched filtering. The SNR is improved at the expense of lower time resolution. Some analysists like to say "not all of the amplitude filtering occurs at the receiver; the amplitude part of the matched filter is evenly divided between the transmitter and the receiver; the cascade of the two filters will result in the correct amplitude matched filtering". Therefore after phase-only matched filtering, the waveform is sometimes called "half-amplitude, full-phase" matched filtered. The optional amplitude filtering at the receiver completes the complete matched filter.

The receiver filter output for the designed waveform and the desired waveform (one with an exact raised-cosine power spectrum) will be compared. Two designed waveforms will be analyzed, the waveform design without the de-rippling step and the waveform design with the de-rippling step.

Figure 33a shows the matched filter output of the designed waveform (solid) and the corresponding waveform without removal of spectral ripples (dashed). This plot is across the entire period. A dotted curve representing the matched output of a desired signal having an exact raised-cosine power spectrum is almost completely
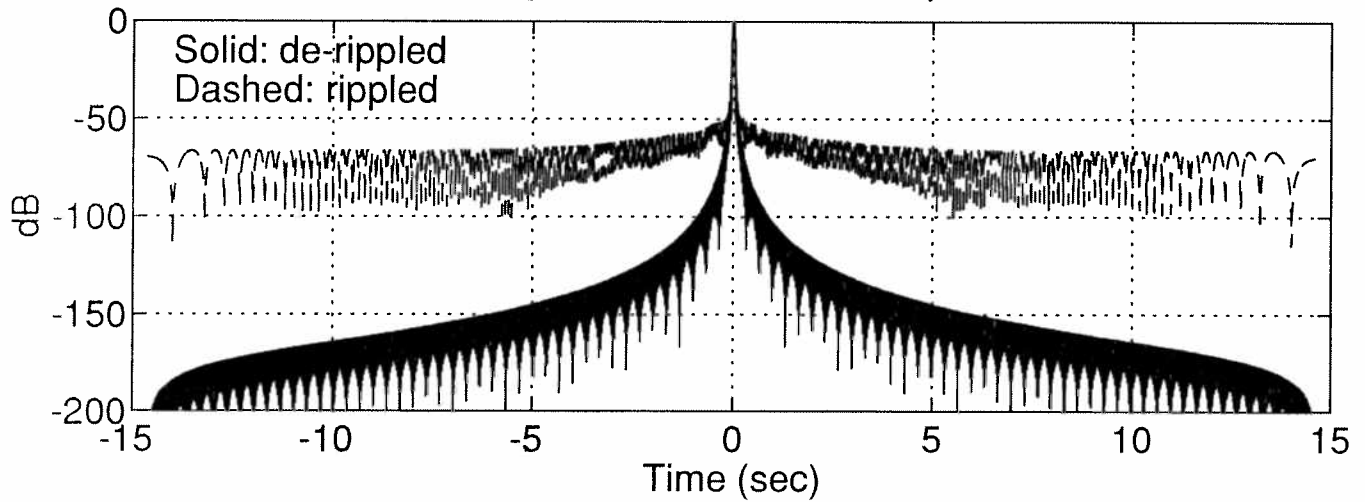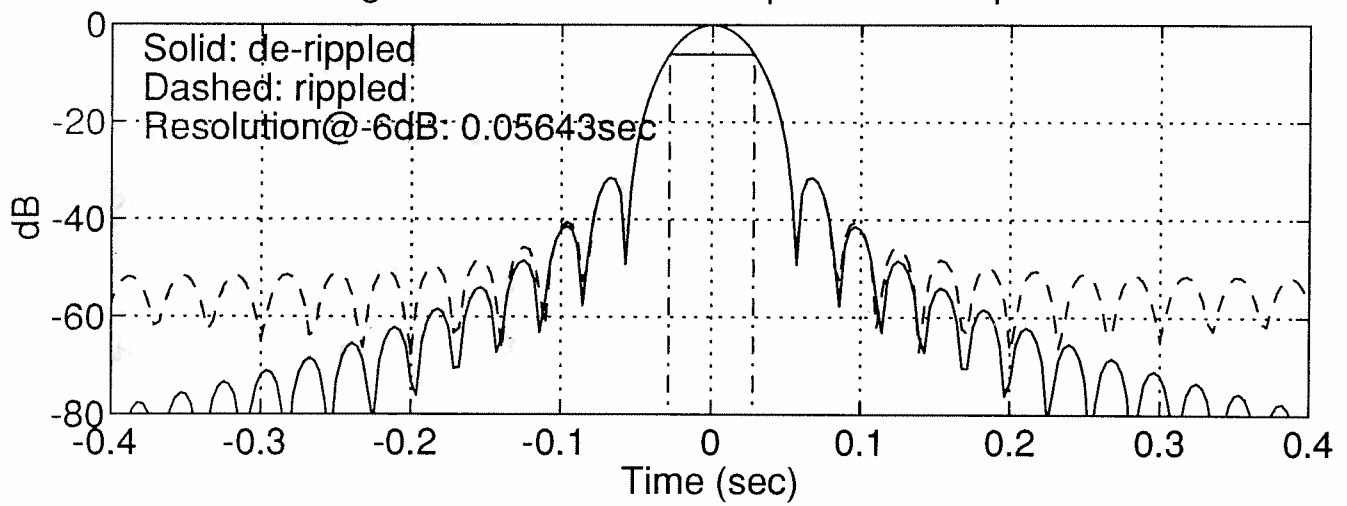
50

Fig.33a: Matched filter output

Fig.33b: Matched filter output: a close-up view

overlapped by the designed signal because their power spectra are almost identical, as was shown in Figures 23 and 24. On the other hand, the error in the rippled spectrum (see Figure 14) effectively raises the time-domain sidelobes, thus necessitates the ripple removal. However the spectral ripples have little effect on the main lobe. In both rippled and de-rippled cases, the time-domain sidelobes fall off in a well behaved manner and do not have any undesirable spikes away from the main lobe. Figure 33b shows a close-up of the main lobes of the rippled and de-rippled cases, which are almost identical. The time resolution, measured at the half height, is 0.05643 seconds.

Figure 34a shows the output after phase only matched filtering across the entire period for the rippled (dashed) and de-rippled (solid) waveforms. As in Figure 33a, a dotted curve representing the phase-only filter output of a desired signal having an exact raised-cosine power spectrum is almost completely overlapped by the designed. The error in the rippled spectrum also raises the time-domain sidelobes, but does not have a significant effect on the main lobe. In both cases, the time-domain sidelobes fall off in a well behaved manner and do not have any undesirable spikes away from the main lobe. Figure 34b shows a close-up of the main lobe of the output after phase-only matched filtering for the rippled and de-rippled cases, which are almost identical. The time resolution, measured at the half height, is 0.045 seconds, which is better than the complete matched filter (.056 sec) as expected. The time resolution was improved at the expense of the time-domain sidelobes increasing by approximately 7 dB. This 7dB cost can be more viewed by comparing Figures 33b and 34b. In the anticipated application the peak SNR will be 20 to 30 dB, so these sidelobe level distinctions are negligible.
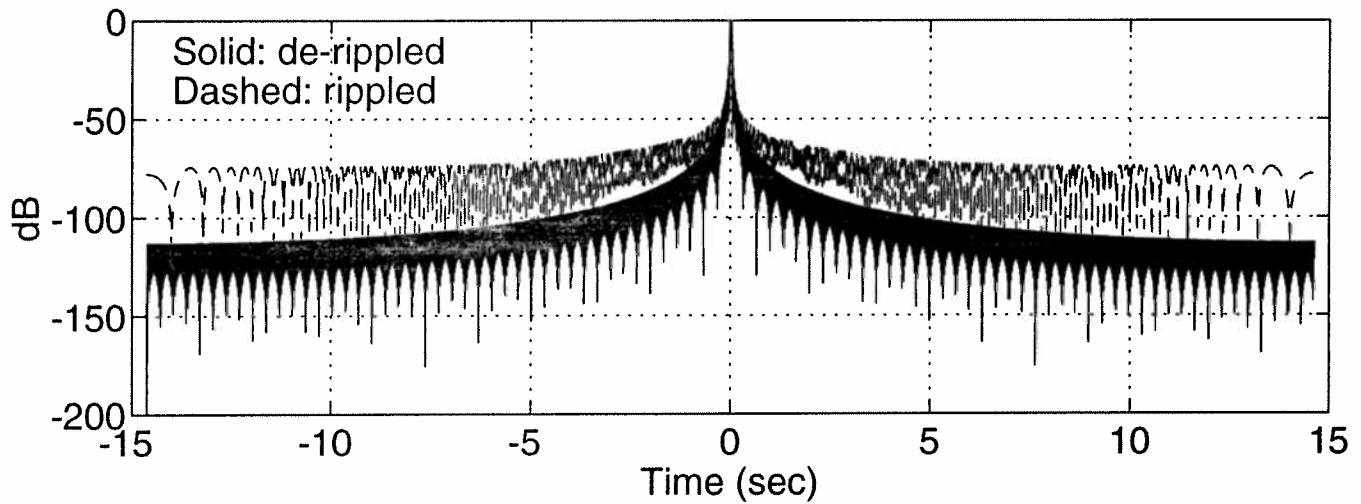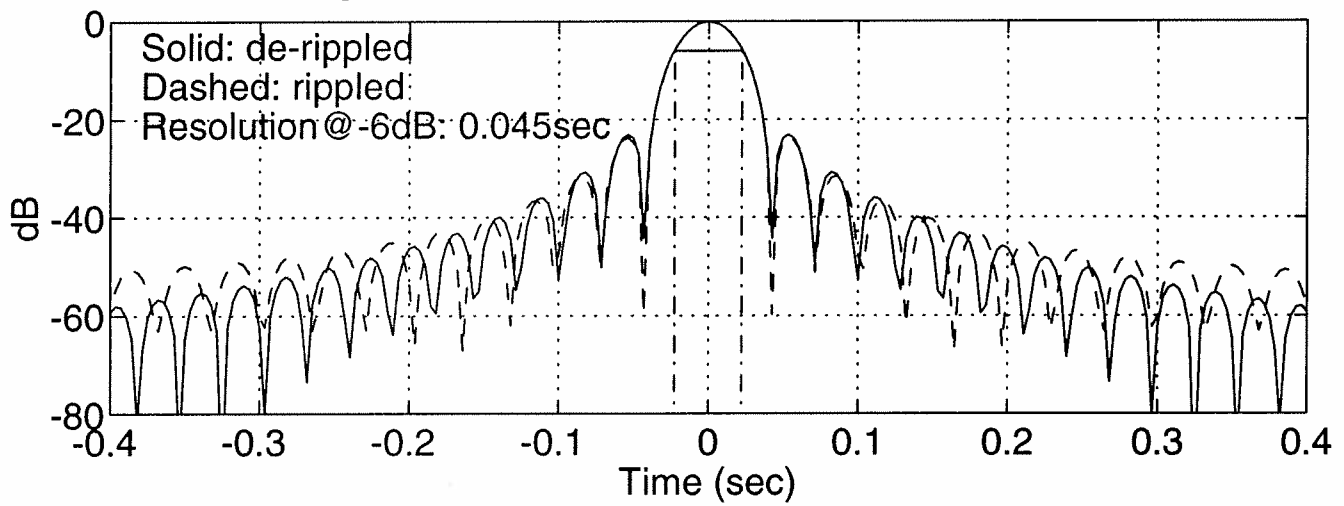
Fig.34a: Phase-only filter output

Solid: de-rippled
Dashed: rippled

Fig.34b: Phase-only filter output: a close-up view

Solid: de-rippled
Dashed: rippled
Resolution @ -6dB: 0.045sec

A disadvantage of using a chirped FM waveform is the waveform's inherent intolerance to Doppler. The ambiguity diagram for chirped waveforms has a diagonal ridge so that a shift in Doppler corresponds to a deviation in estimated time-of-arrival. Figure 35a shows the effect of a Doppler "shift" of 0.034 Hz at 60 Hz and 0.053 Hz at 94Hz (which corrresponds to a source-receiver velocity of 1.65 knots) on the rippled AM nonlinear-FM waveform. The solid and dashed curves are matched filter outputs of the rippled signal with and without Doppler, respectively. The received waveform would be detected to have a time-of-arrival deviating by approximately 0.02 seconds compared to the same waveform without Doppler. The imposed Doppler broadens the main lobe and thus degrades the time-resolution as well. Figure 35b shows the same effect for the de-rippled waveform.

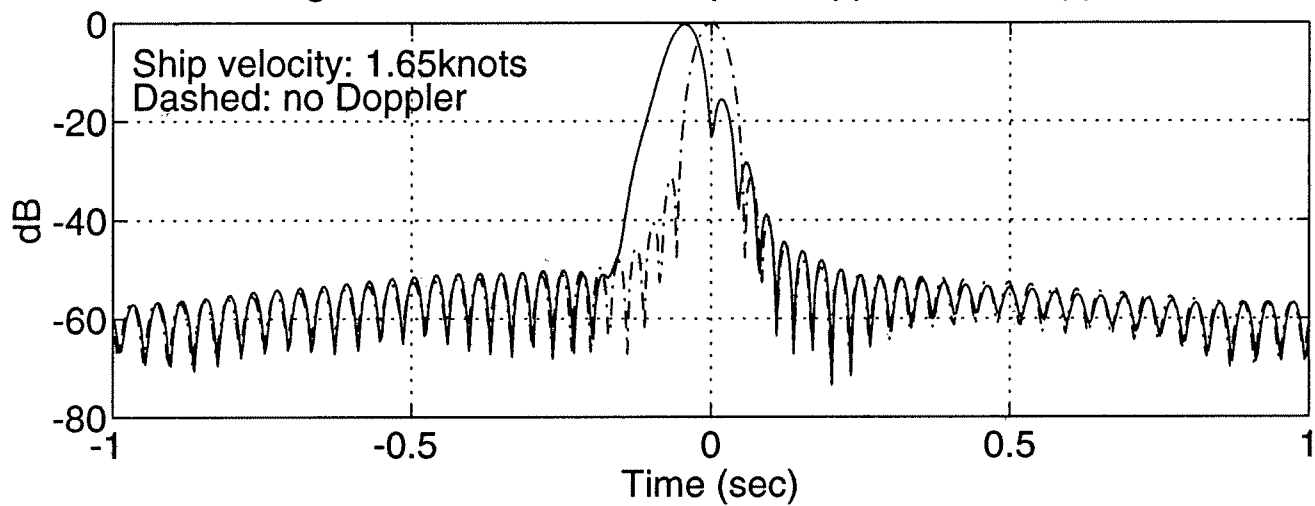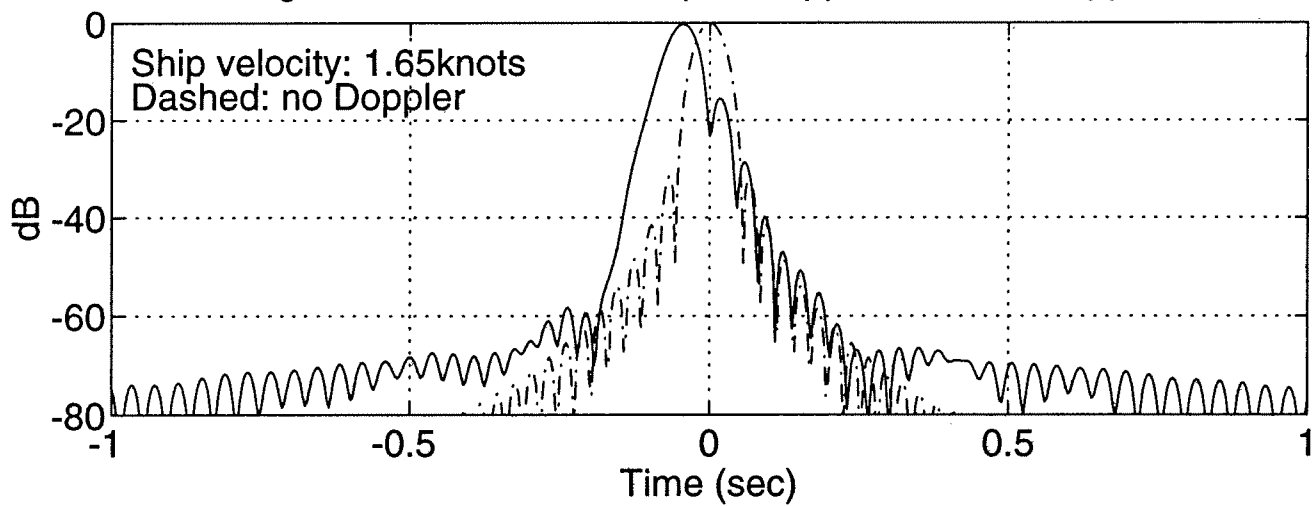Fig.35a: Matched filter output: Doppler effect, rippled

Ship velocity: 1.65knots
Dashed: no Doppler

Fig.35b: Matched filter output: Doppler effect, de-rippled

Ship velocity: 1.65knots
Dashed: no Doppler

Figures 36a and 36b show a comparison of the Doppler effects on the rippled and de-rippled waveforms. It is seen that when the Doppler is present, for both waveforms, the main lobes are practically the same. But the lower order sidelobes in the de-rippled case are considerably lower than in the rippled case. On the other hand, the high order sidelobes in the de-rippled case are raised, approaching the case of the rippled waveform. This is in contrast to the Doppler free cases.

In any case, a Doppler shift does not cause any spurious peaks in the matched filter output away from the main lobe.
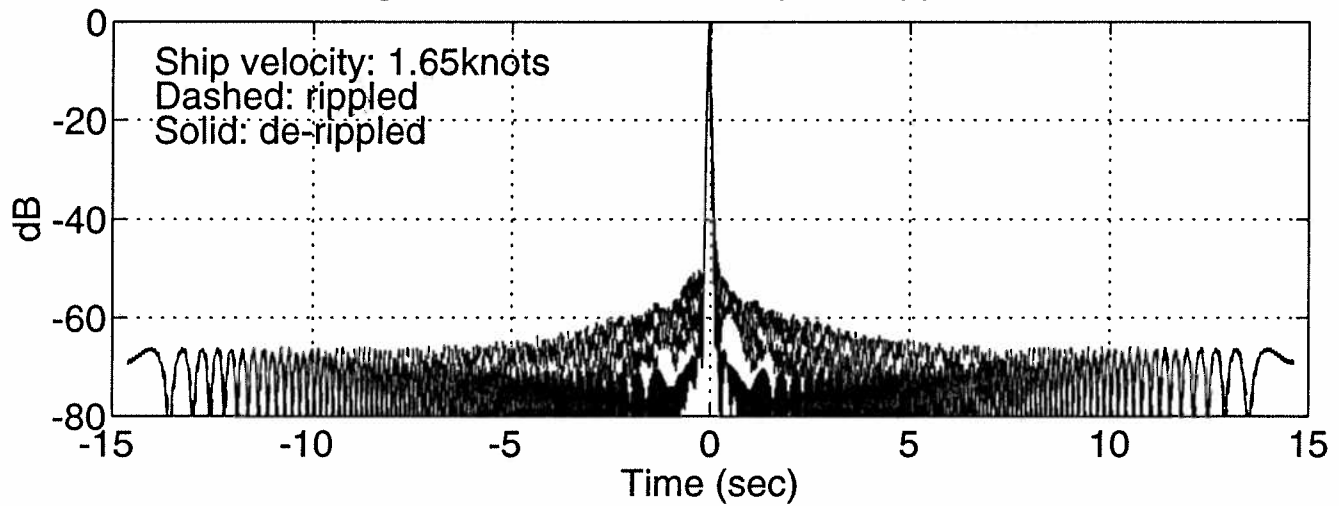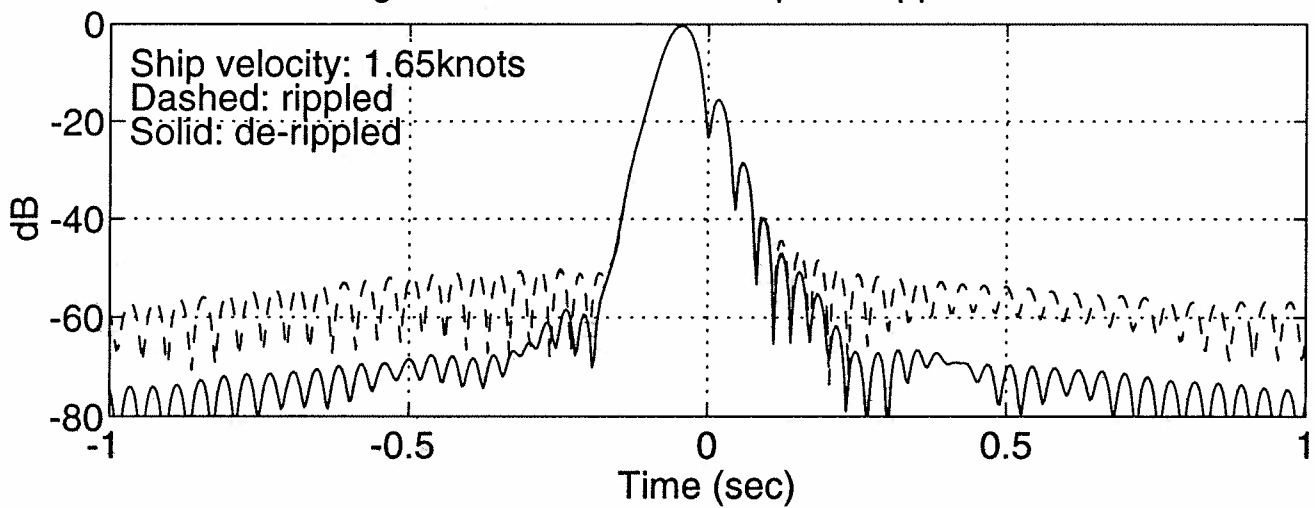
Fig.36a: Matched filter output: Doppler effect

Fig.36b: Matched filter output: Doppler effect

Appendix A

The circuit diagram which models the cable, tuner, and transducer is shown in Figure A-1. Alliant Technologies supplied this circuit diagram along with the element values to the Underwater Sound Group at the University of Michigan (US UMICH). This circuit was used for all of the results in this report. Although, the model was refined by Alliant, our needs are met using this August-5-93 model. The mechanical parts of the transducer are mapped into the circuit using the electro-mechanical equivalent elements.

The input voltage signal is applied to the input of the cable and the resulting pressure output (delivered into the water) complex spectrum is

$$PRESSURE(f) = -j\sqrt{\frac{\rho c}{4\pi} Re[Z_{rad}(f)]} \, I_{out}(f) \qquad (1)$$

The output power spectrum (in μPa, 1 meter from the projector) is simply the squared magnitude of the pressure output complex spectrum, $PRESSURE(f)$.

The radiation impedance, Z_{rad}, is a function of frequency and is accurately approximated as

$$Z_{rad}(f) = 3.221961 \, f^2 + j \, 2508.714 \, f \qquad (2)$$

The crystal voltage and stress are clearly marked in the Figure A-1. The input signal is propagated through the linear time-invariant system using an ABCD matrix approach. Since the transfer function cannot be easily derived, the ABCD matrix approach will be the best route and is described next. For a circuit with a common ground, each circuit element, whether in shunt or in parallel can be represented using

58

a transmission matrix. The transmission matrix relates input and output.

$$\left(\begin{array}{c} V_{in} \\ I_{in} \end{array} \right) = \left(\begin{array}{cc} A & B \\ C & D \end{array} \right) \left(\begin{array}{c} V_{out} \\ I_{out} \end{array} \right) \qquad (3)$$

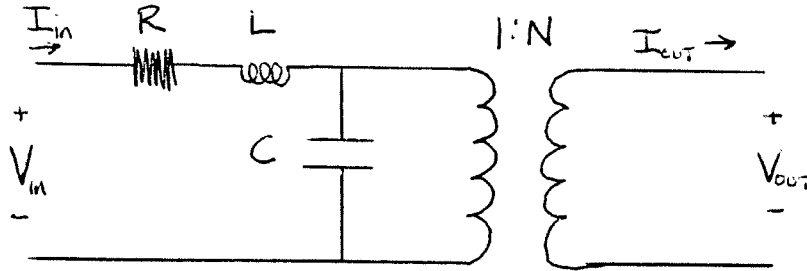where the four elements of the transmission matrix are:

A = voltage gain

B = impedance

C = admittance

D = current gain

With this approach, a ladder (common ground) network can be modelled as a product of elementary ABCD matrices, also called transmission matrices. Notice, the computation must be carried out at each eigenfrequency (one frequency at a time). An example of a few elementary transmission matrices for a series element, shunt element, and ideal transformer are shown below here.

$$T_1 = \left(\begin{array}{cc} 1 & R+j\omega L \\ 0 & 1 \end{array} \right) ; \ T_2 = \left(\begin{array}{cc} 1 & 0 \\ j\omega C & 1 \end{array} \right) ; \ T_3 = \left(\begin{array}{cc} \frac{1}{N} & 0 \\ 0 & N \end{array} \right) \qquad (4)$$

$$\left(\begin{array}{c} V_{in} \\ I_{in} \end{array} \right) = T_1 T_2 T_3 \left(\begin{array}{c} V_{out} \\ I_{out} \end{array} \right) \tag{5}$$

With this method, the current or voltage at any point in the circuit can be calculated by only considering the applicable transmission matrices. To calculate the output voltage and current given the input voltage and current, simply compute the inverse of the aggregate transmission matrix and left-side multiply on both sides of equation (5).
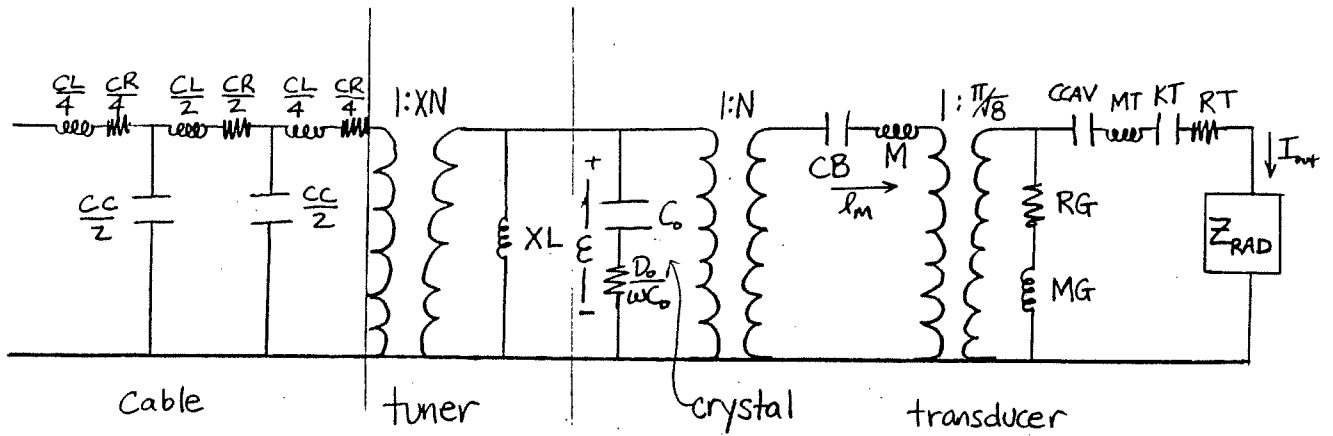
Figure A-1

$D_o = 0.01$

$C_o = 3.312541E - 06$

$N = -9.739412$

$CB = 1.451851E - 08$

$M = 414.09$

$RG = 15358.42$

$MG = 8065.17$

$CCAV = 0.1075355/pressure[Pa]$

$Stress = s_1\,\epsilon + s_2\,lm$ (peak when RMS driven)

$s_1 = 0.401368$

$s_2 = 4594350/j\omega$

$MT = 58.47744$

$KT = 6.08357247E - 08$

$RT = 1.132107E07/\omega$

$XN = 2.0$

$XL = 0.94H$

$CL/mile = 0.00041H/mile$

$CR = /mile = 3.12\Omega/mile$

$CC/mile = 2.1E - 07F/mile$

$power = |I^2|R_{rad} = \frac{4\pi p^2}{\rho c}$

$p = pressure$

$R_{rad} = \mathrm{Re}[Z_{rad}]$